

**REPUBLIC OF TURKEY
SİİRT UNIVERSITY
INSTITUTE OF SCIENCE**

**DESIGN AND IMPLEMENTATION OF MINIATURIZED
ANTENNAS FOR WIRELESS COMMUNICATIONS**

MASTER DEGREE THESIS

**Revink Masoud ABDULHAKIM
(153111012)**

Department of Electrical and Electronics Engineering

**Supervisor: Assist. Prof. Dr. Musa ATAŞ
Co-Supervisor: Dr. Yasser A. FADHEL**

**AUGUST-2017
SİİRT**

THESIS ACCEPTANCE AND APPROVAL

A thesis study titled “ **Design And Implementation of Miniaturized Antennas for Wireless Communications** ” prepared by **Revink Masoud ABDULHAKIM** was accepted as a Master's Degree by Siirt University Institute of Science and Technology, Department of Electrical and Electronics Engineering on 17/08/2017 by the following examining committee.

Examining Committee Members

Signature

Supervisor

Assist. Prof. Dr. Musa ATAŞ

.....

Member

Assist. Prof. Dr. Volkan Müjdat TIRYAKI

.....

Member

Assist. Prof. Dr. Musa ÇIBUK

.....

I confirm the above result.

Assoc. Prof. Dr. Koray ÖZRENK
Director of Institute of Science

THESIS NOTIFICATION

This thesis, which is prepared in accordance with the thesis writing rules, complies with the scientific code of ethics, in case of exploitation of others' works it is referred to in accordance with the scientific norms, innovations contained in the thesis and the results were taken from somewhere else, I declare that any part of the thesis that there is no tampering with the used data is not presented as another thesis work at this university or another university.

Signature

Revink Masoud ABDULHAKIM

Note: In this thesis, the use of original and other source notifications, tables, figures and photographs without reference, it is subject to the provisions of Law No. 5846 on Intellectual and Artistic Works.

ACKNOWLEDGEMENT

Firstly, I wish to express my great acknowledgement to my supervisor Assist. Prof. Dr. Musa ATAŞ and my co-supervisor Dr. Yasser A. FADHEL for their endless support, which shows great interest in my research and valuable feedback, directing and enforcement that i get it from them.

Special thanks and respect are due to the Heads of the Electrical and Electronics Engineering Department of Siirt University, Assoc. Prof. Dr. Fevzi HANSU, Also special thanks to the Head of the Electrical and Computer Engineering Department of University of Duhok (UoD) Dr. Lokman Hadi HASSAN, for his generous help in the provision of measuring devices.

I wish to thank the Electrical and Computer Engineering Department staff of UoD for their advice and kind help. Special thanks go to my friends and wonderful colleagues. Finally, I would like to thankfulness to my parents for their longanimity, enforcement and great support in every way.

Revink Masoud ABDULHAKIM
SIIRT-2017

CONTENTS

	<u>Page</u>
ACKNOWLEDGMENT	iii
CONTENTS	iv
LIST OF TABLES	vi
LIST OF FIGURES	vii
LIST OF ABBREVIATIONS AND SYMBOLS	ix
ABSTRACT	xi
ÖZET	xii
1. INTRODUCTION	1
1.1. Aim of the Work.....	1
1.2. Thesis Objective.....	2
1.3 Thesis Contribution.....	2
1.4 Thesis Organization.....	2
2. LITERATURE RESEARCH	3
2.1. General Antenna Characteristics.....	4
2.1.1. Radiation Pattern.....	4
2.1.2. Directivity.....	6
2.1.3. Gain.....	7
2.1.4. Antenna Efficiency.....	7
2.1.5. Input Impedance.....	9
2.1.6. Reflection Coefficient.....	9
2.1.7. Bandwidth (BW).....	10
2.2. Microstrip Antennas.....	11
2.3. Main Types of Miniaturized Antenna.....	11
2.3.1 Multiband Fractal Antennas.....	12
2.3.2. Slot Antennas (SA).....	13
2.4 Radio-Frequency Identification (RFID) Antennas (Application Example).....	16
3. MATERIAL AND METHODS	19
3.1. Material.....	19
3.2. Methods.....	22
3.2.1. Miniaturization of a Planar Strip-Shaped Monopole Antenna (PSSMA) for WLAN Application.....	22
3.2.1.1. Antenna Design.....	23
3.2.1.2. Miniaturization.....	25
3.2.2. Miniaturization of a Planar Circular Monopole Antenna (PCMA) for WLAN Application.....	27
3.2.2.1. Antenna Design.....	29
3.2.2.2. Miniaturization.....	30

4. RESULTS AND DISCUSSION	33
4.1. Miniaturization of a Planar Strip-Shaped Monopole Antenna (PSSMA) for WLAN Application	33
4.2. Miniaturization of a Planar Circular Monopole Antenna (PCMA) for UWB Application.....	41
5. CONCLUSIONS AND FUTURE WORKS	53
5.1. Conclusions	53
5.2. Future Works	54
6. REFERENCES	55
CURRICULUM VITAE	58



LIST OF TABLES

	<u>Page</u>
Table 3.1. Design parameter of PSSMA	24
Table 3.2. Design parameter of corrugated PSSMA.....	25
Table 3.3. Design parameter of meandered PSSMA	26
Table 3.4. Design parameter of PCMA	30
Table 3.5. Design parameter of PCSMA.....	31
Table 3.6. Design parameter of corrugated PCMA.....	32



LIST OF FIGURES

	<u>Page</u>
Figure 2.1. Antenna analysis by coordinate system	4
Figure 2.2. The normalized two-dimensional radiation pattern with a spacing $d = 0.25 \lambda$ of a 10-element linear array (a) linear field pattern, (b) linear power pattern, (c) power pattern in dB (Balanis, 2005).....	5
Figure 2.3. Bandwidth measuring from the curve of reflection coefficient.....	10
Figure 2.4. Configuration of Microstrip antenna.....	11
Figure 2.5. Fractal Sierpinski gasket monopole antenna (a) First iteration (b) Fourth iteration	13
Figure 2.6. The Sierpinski gasket measured return loss with fourth iteration over a frequency range of (50 MHz to 12 GHz)	13
Figure 2.7. (a) Waveguide slot antenna. (b) Simple slotted-cylinder antenna.....	14
Figure 2.8. Rectangular slot.....	14
Figure 2.9. A typical passive RFID tags with antenna.....	16
Figure 2.10. Smart watches Antenna Structures of (a) Dipole antenna (b) Monopole antenna.....	17
Figure 3.1. Overview of CST Microwave Studio Software Package	19
Figure 3.2. FR4 copper PCB boards.....	19
Figure 3.3. The Vector Network Analyzer Rohde & Schwarz® ZVL13 with frequency range of (9kHz ~ 13.6 GHz)	20
Figure 3.4. The Measurement Setup, (a) Perspective view, (b) Layout view	21
Figure 3.5. Geometry of the simulated PSSMA	24
Figure 3.6. Geometry of the simulated corrugated PSSMA.....	25
Figure 3.7. Geometry of the simulated meandered PSSMA	26
Figure 3.8. Geometry of the simulated PCMA	30
Figure 3.9. Geometry of the simulated PCSMA.....	31
Figure 3.10. Geometry of the simulated corrugated PCMA.....	32
Figure 4.1. Comparison of simulated return loss curves for the PSSMA, corrugated PSSMA, and meandered PSSMA.....	34
Figure 4.2. PSSMA surface current distribution at 2.45 GHz	35
Figure 4.3. Corrugated PSSMA surface current distribution at 2.45 GHz	35
Figure 4.4. Meandered PSSMA surface current distribution at (a) 2.45 GHz, and (b) 5.5 GHz	36
Figure 4.5. Fabricated PSSMA	37
Figure 4.6. Fabricated corrugated PSSMA	37
Figure 4.7. Fabricated meandered PSSMA.....	37
Figure 4.8. Simulated and measured curves of return loss for the PSSMA.....	38
Figure 4.9. Simulated and measured curves of return loss for the corrugated PSSMA	38
Figure 4.10. Simulated and measured curves of return loss for the meandered PSSMA	38
Figure 4.11. Radiation patterns measured (—) and simulated (---) of the PSSMA in E and H planes, at frequency of 2.45 GHz.....	39
Figure 4.12. Radiation patterns measured (—) and simulated (---) of the corrugated PSSMA in E and H planes, at frequency of 2.45 GHz.....	39
Figure 4.13. Radiation patterns measured (—) and simulated (---) in of the meandered PSSMA in E and H planes, at the two frequencies 2.45 and 5.5 GHz.....	40
Figure 4.14. Comparison of simulated realized gain curves for PSSMA, corrugated PSSMA and meandered PSSMA	41

Figure 4.15. Comparison of simulated return loss curves for PCMA, PCSMA and corrugated PCMA	42
Figure 4.16. PCMA surface current distribution at (a) 5GHz, and (b) 9 GHz.....	43
Figure 4.17. PCSMA Surface current distribution at (a) 5 GHz, and (b) 9 GHz	44
Figure 4.18. Corrugated PCMA surface current distribution at (a) 5 GHz, and(b) 9 GHz	45
Figure 4.19. Fabricated PCMA.....	46
Figure 4.20. Fabricated PCSMA	46
Figure 4.21. Fabricated corrugated PCMA.....	46
Figure 4.22. Simulated and measured curves of return loss for the PCMA	47
Figure 4.23. Simulated and measured curves of return loss for the PCSMA.....	47
Figure 4.24. Simulated and measured curves of return loss for the corrugated PCMA.....	47
Figure 4.25. Radiation patterns simulated (---) and measured (—) of the PCMA in H and E planes, at frequency of 5 and 9 GHz	48
Figure 4.26. Radiation patterns simulated (---) and measured (—) of the PCSMA in H and E planes, at frequency of 5 and 9 GHz.....	49
Figure 4.27. Radiation patterns simulated (---) and measured (—) of the corrugated PCMA in H and E planes, at frequency of 5 and 9 GHz	50
Figure 4.28. Comparison of simulated realized gain curves for the PCMA, PCSMA and corrugated PCMA	51

LIST OF ABBREVIATIONS AND SYMBOLS

<u>Abbreviation</u>	<u>Explanation</u>
WLAN	: Wireless Local Area Network
UWB	: Ultra-Wide Band
CST	: Computer Simulation Technology
FR4	: Fiberglass Reinforced epoxy laminated
PCB	: Printed Circuit Boards
DMS	: Defected Microstrip Structure
DGS	: Defected Ground Structure
PSSMA	: Planar Strip-Shaped Monopole Antenna
PCMA	: Planar Circular Monopole Antenna
PCSMA	: Planar Crescent-Shaped Monopole Antenna
Wi-MAX	: Worldwide Interoperability for Microwave Access
HPBW	: Half Power Beam Width
VSWR	: Voltage standing-wave ratio
BW	: Bandwidth
ABW	: Absolute Bandwidth
FBW	: Fractional Bandwidth
FCC	: Federal Communications Commission
UHF	: Ultra-High Frequency
RFID	: Radio Frequency Identification
RF	: Radio Frequency
MNG	: μ -Negative metamaterials
TSA	: Tapered Slot Antenna
VNA	: Vector Network Analyzer
Tx Ant	: Transmitter Antenna
Rx Ant	: Receiver Antenna
SMA	: Sub Miniature version A
SA	: Slot Antenna
WSA	: Waveguide Slot Antenna
UoD	: University of Duhok

<u>Symbol</u>	<u>Explanation</u>
λ	: Lambda (wave length)
θ	: Theta (elevation angle)
ϕ	: Phi (azimuth angle)
ϵ_r	: Dielectric constant
c	: Speed of light
π	: Pi
D	: Directivity (dimensionless)
D_0	: Maximum directivity (dimensionless)
e_c	: Conduction efficiency (dimensionless)
e_d	: Dielectric efficiency (dimensionless)
E_r	: Field intensities of the reflected waves from a plane screen of infinite Extent
e_{ref}	: Reflection (mismatch) efficiency = $(1 - k ^2)$ (dimensionless)
e_t	: Total efficiency (dimensionless)
f_L	: Lower limit of frequency
f_U	: Upper limit of frequency
F_s	: The field behind the screen
F_{cs}	: The field behind the complementary screen
F_o	: The field with no screen
G	: Gain of the antenna
G_0	: Conductance
k	: Reflection coefficient
P_{rad}	: Total radiated power (W)
R_{in}	: Input resistance of the antenna
RL	: Returned loss or returned power ratio
U	: Radiation intensity (W/unit solid angle)
U_0	: Isotropic source radiation intensity (W/unit solid angle)
U_{max}	: Maximum radiation intensity (W/unit solid angle)
V_i	: Incident voltage wave
V_r	: Reflected voltage wave
X_{in}	: Input reactance of the antenna
Y_0	: Characteristic admittance
Y_1	: Shunt admittance
Z_0	: Characteristic impedance
Z_1	: Impedance surface of the screen
Z_2	: Impedance surface of the complementary metal screen
Z_A	: Input impedance of the antenna
μ	: Permeability
σ	: Conductivity
λ_{eff}	: Effective wavelength

ABSTRACT

M.Sc. THESIS

DESIGN AND IMPLEMENTATION OF MINIATURIZED ANTENNAS FOR WIRELESS COMMUNICATIONS

Revink Masoud ABDULHAKIM

**The Graduate School of Natural and Applied Science of Siirt University
The Master Degree of Science
in Electrical and Electronics Engineering**

Supervisor : Assist. Prof. Dr. Musa ATAŞ

Co-Supervisor : Dr. Yasser A. FADHEL

2017, 57 Pages

Miniaturization of planar microstrip antennas have been investigated. Different techniques have been applied to design miniaturized antennas serving for wireless communication systems. These techniques were inspired from understanding the common features of planar antennas and the requirements of these antennas to be working at certain frequencies like Wireless Local Area Network (WLAN) antennas or even covering wider range of frequencies such as Ultra-Wide Band (UWB) antennas, meanwhile keeping its properties almost unchanged.

In this work, the design techniques of these antennas were emphasized, and how is it possible to have smaller size with same characteristics. The essential idea is to enable excitation current to follow the same path length as required in the full size antenna within smaller size in the miniaturized structure. Corrugating and meandering were used as two main techniques that fulfil the requirements. Another technique of eliminating the least excited areas of the planar antennas was also introduced. The location of these areas has been determined by simulating the surface current distribution of the full size antenna before miniaturization process. All of the designed antennas have been simulated by CST Microwave Studio 2014, and they have been fabricated on FR4 PCB boards then tested via practical measurements by using Rohde & Schwarz® ZVL13 Vector Network Analyzer.

Simulation and measured results shown a good agreement, and confirming the validation of the techniques being used. In addition, the suggested techniques succeeded to miniaturize the overall size of Planar Strip-Shaped Monopole Antenna (PSSMA) serving WLAN applications, by (10.7%) of the original antenna size for Corrugated PSSMA and (14.28%) for Meandered PSSMA. Also enables miniaturization of the overall size of Planar Circular Monopole Antenna (PCMA) by (11.8%) of the original antenna size for Planar Crescent-Shaped Monopole Antenna (PC SMA), and (42.6%) for Corrugated PCMA while still covering the UWB frequency range. Although the reduction in Corrugated PCMA is huge but results shown that its gain still higher than 2 dB which is comparable to the traditional half-wave dipole gain.

Keywords: Miniaturized Antennas, WLAN Antenna, UWB Antenna, Strip-Shaped Antenna, Meandering, Corrugation, PCMA, Crescent-Shaped Antenna.

ÖZET

YÜKSEK LİSANS TEZİ

KABLOSUZ HABERLEŞME İÇİN MİNYATÜRE ANTENLERİN TASARIMI VE UYGULANMASI

Revink Masoud ABDULHAKIM

**Siirt Üniversitesi Fen Bilimleri Enstitüsü
Elektrik-Elektronik Mühendisliği Anabilim Dalı**

Danışman : Yrd.Doç.Dr. Musa ATAŞ

II. Danışman : Dr. Yasser A. FADHEL

2017, 57 Sayfa

Düzlemsel mikroşerit antenlerin minyatürleştirilmesi araştırılmıştır. Kablosuz iletişim sistemleri için minyatür anten tasarımı için farklı teknikler uygulanmıştır. Bu teknikler, düzlemsel antenlerin ortak özelliklerini ve bu antenlerin Kablosuz Yerel Ağ (KYA) antenleri gibi belirli frekanslarda çalışmasını veya Ultra Geniş Bantlı (UGB) antenler gibi daha geniş frekans aralıklarında özelliklerini hiç değiştirmeden koruyacak bir algıdan esinlenmiştir.

Bu çalışmada, söz konusu antenlerin tasarım teknikleri vurgulanmış ve aynı özelliklere sahip daha küçük boyutta bir anten nasıl elde edilebilir araştırılmıştır. Temel fikir, uyarma akımının minyatür yapıda daha küçük boyutta tam boyutlu antende gerekli olan aynı yol uzunluğunu izlemesini sağlamaktır. Gereksinimleri karşılayan iki temel yöntem olarak oluklu ve kıvrımlı türler kullanılmıştır. Ayrıca, düzlemsel antenlerin en az ilgi çeken kısmını ortadan kaldıran diğer bir teknik de tanıtılmıştır. Bu alanların konumu, minyatürizasyon işleminden önce tam boyutlu antenin yüzey akım dağılımının benzetimiyle belirlenmiştir. Tasarlanan tüm antenler CST Microwave Studio 2014 tarafından simüle edilmiş, FR4 PCB panolarında üretimleri yapılmış ve Rohde & Schwarz® ZVL13 Vektör Network Analizör ile test edilmiştir.

Simülasyon ve ölçülen sonuçlar kendi aralarında mutabık kalarak kullanılan yaklaşım doğrulanmıştır. Buna ek olarak, önerilen yaklaşım, KYA uygulamalarındaki Düzlemsel Şerit Şekilli Monopole Anten (DŞŞMA)'in genel boyutlarını, oluklu DŞŞMA için orijinal anten boyutunun (%10.7) ve Kıvrımlı DŞŞMA için de (% 14.28) minyatürize etmeyi başarmıştır. Ayrıca UGB frekansı sınırları içinde kalmak suretiyle Düzlemsel Hilal şeklindeki Monopole Anten (DHMA) için Düzlemsel Dairesel Monopol Anten (DDMA) boyutunun (% 11.8) ve Oluklu PCMA için de (% 42.6) minyatürize edilmesine olanak tanınmıştır. Oluklu PCMA'daki azalma oldukça büyük olmasına rağmen sonuçlar, kazancının geleneksel yarı dalga dipol kazanımı ile karşılaştırılabilir olan 2 dB'den daha yüksek olduğunu göstermiştir.

Anahtar Kelimeler: Minyatür Antenler, KYA Anteni, UGB Anteni, Şerit Şekilli Anten, Kıvrımlı, Oluklu Mukavva, DDMA, Hilal Şekilli Anten.

1. INTRODUCTION

Recently the wireless equipment witnessed a huge reduction in their sizes to be integrated within compact and tiny portable devices and working different bands of frequencies. The challenges are raised up as much as the development in these devices requires more integration and compacting for the microwave components while keeping their performance at high levels.

As already well known that antennas play an essential role in any wireless communication system, wither having a directional or omnidirectional radiation pattern, which depend on the application that being used for. Accordingly, if the application is for radars or imaging systems then directional antennas are required. If it will be used for cellular or personal communication systems then omnidirectional antennas are preferred.

It is very common that antenna length, aspects or edges must have effectively electrical length as much as required by the wavelengths of the desired resonant frequencies employed by the wireless communication devices. Among the vast number of existing types of antennas microstrip antennas are chosen for this difficult task.

In this research, microstrip planar antennas have been fabricated and designed practically. The operational frequency range for the antenna designed here were varied between single band frequency (2.45 GHz), dual band of frequencies (2.45 GHz & 5.2 GHz) to be used for Wireless Local Area Network (WLAN) and Ultra-Wideband frequency (UWB) to be used for UWB technology systems (3.1~10.6 GHz). Then miniaturized versions of these antennas have been designed according to certain suggested design methods. These methods have been proven to be efficient after maintaining the antenna features almost unchanged, compared to the original antennas.

1.1. Aim of the Work

The aim of the work for this these can be listed as follow:

1. Investigating the different shapes used for miniaturization of antennas.
2. The acquired results of the study will be utilized to achieve more insight into the issue of miniaturized antennas to inspire some new shapes.
3. Some design examples will be simulated and analyzed by known software packages.

1.2. Thesis Objective

In this thesis the objective is oriented on modifying design techniques of planar antennas to suggest efficient methods to get miniaturized antennas while maintaining the characteristics almost unchanged. The main challenge is changing the overall size of these antennas without jeopardizing their properties.

1.3. Thesis Contribution

Some shapes have been suggested for miniaturizing planar WLAN and UWB antennas which inspired from understanding the design procedure and behavior of these antennas. Simulation and measured results shown that these techniques are applicable efficiently not just on the design example introduced here but exceeding to other vast range of antenna shapes.

1.4 Thesis Organization

This thesis is organized in five chapters, as follows:

Chapter two introduces survey on some literatures about the miniaturization of antennas. The basic antenna principles and its general characteristics have also been discussed in this chapter. Then some typical antennas have been mentioned.

Chapter three illustrates the material needed to achieve this research and the suggested method, also contains designing of some planar antennas along with their modification to get miniaturized versions. In general, three different techniques have been suggested; corrugation, meandering, and eliminating the least current distributed areas. These techniques have been exploited to miniaturize the planar-strip shaped monopole antenna (PSSMA) as a WLAN antenna and the planar circular monopole antenna (PCMA) as an Ultra-Wideband UWB antenna.

Chapter four shows the simulation and the practical measurement results for the all designed antennas and their miniaturized versions. The surface current distribution, return loss, gains and radiation pattern are the most important features that have been achieved to assess the efficient of these antennas.

Chapter five contains the conclusions that have been observed from designing of these antennas and their practical implementation and measurements. Also presents suggestions to be worked on as future works.

2. LITERATURE REVIEW

Many scientists competed to record a lead in miniaturizing planar antennas that obey the compact size requirements of nowadays low profile communication systems. For a long time fractal antennas with repeated shapes were used for working on multiple bands of frequencies, whereas in (Singh, 2009) it has been proven that by increasing the fractal dimension of the antenna then higher degree of miniaturization could be achieved, accordingly fractal structure could be used to design low profile and small size antennas.

Others used different shapes and configurations to design miniaturized antennas such as using a split-ring slot antenna (El Misilmani, 2012), which operated on triple-bands of frequencies to be used for WLAN/Wi-MAX applications. Another design used corrugations on the edges of antipodal tapered-slot antenna to get a miniaturized size without jeopardizing its performance that covers the Ultra-wideband (UWB) frequency range (Abbosh, 2009).

A miniaturization up to 45% has been achieved in (Pandhare, 2015) by using defected ground structure (DGS) that shifted the resonance frequency of an elementary microstrip antenna array from (5.2 to 3.8) GHz which is suitable for Wi-Max applications.

Other design added two slots to the ground plane of pentagonal shaped patch monopole antenna which give an extra resonating mode while maintaining miniaturized size (Majeed, 2015). The benefits behind the small size of antenna via meandering of the microstrip fed line was helpful for broadening the band of frequency as in (Fadhel, 2012; Sayidmarie, 2012) where impedance matching has been achieved over a very wide range of frequencies (3.1 ~ 10.6 GHz) which is the entire UWB range.

In this research the corrugation of the edges for radiator element, eliminating of the least current distributed areas and meandering have been proposed as a major effective techniques for miniaturization of WLAN and UWB antennas. Other literature has been mentioned at the starting of the design sections in chapter three, where classified and arranged according to the type of antenna being designed and the techniques of miniaturization that being used.

2.1. General Antenna Characteristics

An antenna (or antenna) is an electrical tool that turns radio waves into electrical power, and vice versa. They are ordinarily used with transmitter radio or receiver radio.

To describe antenna performance, definitions of different parameters are requisite. Some of these factors are interrelated. Therefore, they do not need to be determined to obtain a full explanation of antenna work. Definitions of parameter and main principles of concerned antennas are given in this chapter.

2.1.1. Radiation Pattern

The radiation pattern of an antenna could be defined as a graphical representation of mathematical expression which is a function of space coordinates. The radiation pattern is divided into two main regions according to the coverage distance; nearfield and farfield. The farfield patterns are most important for wireless transmission.

The radiation properties are containing; directivity, power flux density, field strength, radiation intensity, phase or polarization (Balanis, 2005). The radiation patterns are usually represented by two dimensional or three dimensional plotting of the radiated power as a function of observation point along a constant radius. Figure 2.1 shows a typical amplitude radiation pattern as an effect of the received electric or magnetic field at fixed radius. And if the plot is taken for the power density along constant radius then it will be called an amplitude power pattern (Balanis, 2005).

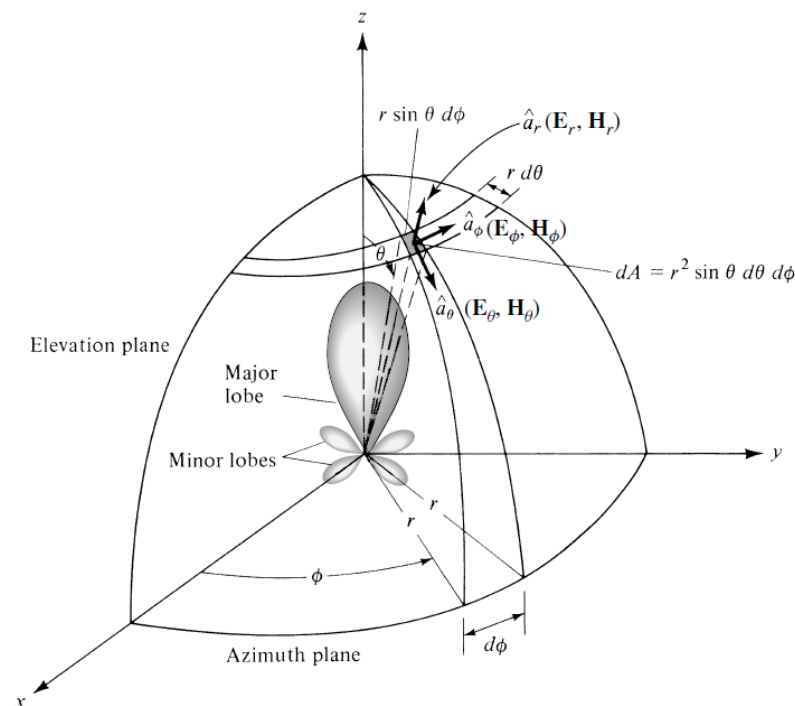


Figure 2.1. Antenna analysis by coordinate system (Balanis, 2005).

The pattern of the two-dimensional (2D) standard field (drawn on a linear), power pattern (drawn on a linear), and power pattern (drawn on a logarithmic dB) scale. The pattern of the two-dimensional standard field (plotted in a linear scale), the power pattern (linearly plotted), the power pattern (drawn on a logarithmic scale) of the linear antenna array consisting of 10 identical elements having a spacing of $d = 0.25\lambda$ between them, as shown in figure 2.2. There are two points relative to the maximum value of the radiation pattern where the pattern reaches its half power (-3 dB points), therefore these two points are named half-power points and the angular width between them is called the half power beam width (HPBW) as illustrated in figure 2.2.

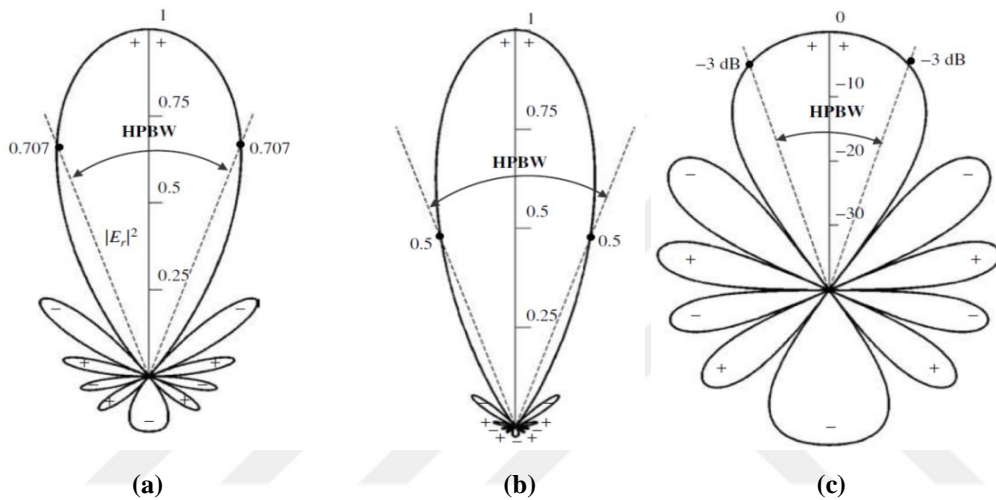


Figure 2.2. The normalized two-dimensional radiation pattern with a spacing $d = 0.25 \lambda$ of a 10-element linear array (a) linear field pattern, (b) linear power pattern, (c) power pattern in dB (Balanis, 2005).

The three-dimensional (3D) pattern has more indication on the power being received or transmitted around the antenna. Plotting of such patterns require measuring and recording a series of two-dimensional (2D) patterns. Each of these 2D-patterns is plotted either as a function of θ while ϕ is kept constant, or as a function of ϕ for particular value of θ .

The suitable distance for observation of the radiation pattern is taken at the far-field (Fraunhofer) region, which is defined as that area of the antenna field where the angular field sharing is basically independent of the distance from the antenna. And it is usually decided to be started at distances greater than $2d^2/\lambda$ from the antenna, where d is the maximum after the antenna is comprehensive, and λ is the wavelength (Balanis, 2005).

Antennas could be classified according to the shape of their radiation patterns, therefore the various antennas can be divided in to the following types (Balanis, 2008):

(a) **Isotropic:** It is an ideal lossless antenna having same radiation in all directions. This hypothetical antenna is often taken as a reference for comparison of the directive gain of other antennas.

(b) **Directional:** An antenna with a radiated electromagnetic wave or receiver feature actively in some directions more than in others. This commonly applies to an antenna with a far more directional antenna than a half-wave dipole antenna.

(c) **Omni-directional:** Antenna has essentially non-directional pattern at a certain plane and pattern of directional at any orthogonal plane.

2.1.2. Directivity

Directivity is a ratio of the radiation intensity for certain antenna in a given direction to the radiation intensity if distributed to overall directions. The radiation intensity average equals to the whole radiated power divided by the whole solid angle of 4π . The maximum radiation intensity direction is implicit while the direction is not particular (Balanis, 2005) as a result; the non-isotropic source directivity is the same for the ratio of the intensity of radiation in a particular direction over the presence of an isotropic source. In mathematical way, it can be written as (Balanis, 2005):

$$D = \frac{U}{U_0} = \frac{4\pi U}{P_{rad}} \quad (2.1)$$

$$D_{max} = \frac{4\pi U_{max}}{P_{rad}} \quad (2.2)$$

Where:

D = directivity (dimensionless)

U_{max} = maximum radiation intensity (W/unit solid angle)

U = radiation intensity (W/unit solid angle)

U_0 = radiation intensity of isotropic source (W/solid angle unit)

P_{rad} = total radiated power (W)

For the isotropic source, and referring to (2.1) or (2.2) it could be concluded that when U , U_0 , and U_{max} have the same values the directivity is unity since.

2.1.3. Gain

The antenna gain (in a given direction) is defined as the ratio of the radiation intensity, in a given direction, to the radiation intensity being radiated isotropically. Unlike the directivity, the gain of antenna is calculated after considering the antenna efficiency as well as its directional capabilities. For the case of the isotropically radiated power, the power accepted (input) is equal to the radiation intensity by the antenna divided by 4π , as given by (Balanis, 2005):

$$\begin{aligned} \text{Gain} &= 4\pi \frac{\text{radiation intensity}}{\text{total input (accepted) power}} \\ &= 4\pi \frac{U(\theta, \phi)}{P_{in}} \text{ (dimensionless)} \end{aligned} \quad (2.3)$$

It is very common to deal with relative gain known as the power gain relationship in a particular direction by gaining the power of a reference antenna in its referenced direction. The input power should be the similar for both antennas. The reference antenna is frequently the horn, dipole, or any other antenna which its gain is known or can be calculated.

2.1.4. Antenna Efficiency

The antenna efficiency (e_t) is used to calculate losses in the input terminals and within the antenna structure. These losses may be attributed to:

1. Reflections resulting from mismatch between the antenna and feeder line.
2. Lost dielectric parts of the antenna and non-perfect conducting metallic parts.

Generally, the overall efficiency can be expressed as (Balanis, 2005):

$$e_t = e_{ref} e_c e_d \quad (2.4)$$

Where:

e_t = total efficiency (dimensionless)

e_{ref} = reflection (mismatch) efficiency = $(1 - |k|^2)$ (dimensionless)

e_c = conduction efficiency (dimensionless)

e_d = dielectric efficiency (dimensionless)

k = voltage reflection coefficient at the input terminals of the antenna.

Normally e_d and e_c are very hard to calculate, but can be empirically determined. Even through the measurements, they cannot be divided, typically more appropriate to write (2.4) as follows:

$$e_t = e_{ref} e_{cd} = e_{rad}(1 - |k|^2) \quad (2.5)$$

Where $e_{rad}=e_{cd}= e_c e_d$ = radiation efficiency of an antenna, which is used to linked the directivity and gain.

The total radiated power (P_{rad}) is related to the total input power (P_{in}) by (Balanis, 2005):

$$P_{rad} = e_{rad}P_{in} \quad (2.6)$$

The gain G also is associated to the directivity D by (Balanis, 2005):

$$G = e_{rad}D \quad (2.7)$$

2.1.5. Input Impedance

The input impedance can be described as the impedance introduced by an antenna at its the ratio or terminals of the suitable components of the electric to magnetic fields at the ratio of the voltage to current or a point at a pair of terminals (Balanis, 2005).

The input impedance is collected of the following parts real and imaginary (Stutzman, 1981):

$$Z_{in} = R_{in} + jX_{in} \quad (2.8)$$

Where:

R_{in} = input resistance, real part and represents dissipation

X_{in} = input reactance, imaginary part and represents the stored power in the near antenna field.

2.1.6. Reflection Coefficient

The input impedance discussed in the previous section is very essential to be matched to that of the feeder section; otherwise severe reflections will be taken place. The input impedance is compared with relation to the source features impedance or transmission line. As if both are unequal, then a voltage wave scaled by k factor is reflected, where the reflection coefficient of voltage is called k and given by (Milligan, 2005):

$$k = \frac{Z_A - Z_0}{Z_A + Z_0} \quad (2.9)$$

Where:

Z_A = the input impedance of the antenna

Z_0 = the measurement characteristic impedance for the transmission line.

Existing of two opposite directed waves (*i.e.* incident and reflected) which will be interfered with each other to perform a new waveform called the standing-wave, so if the wave is voltage wave then it is named the voltage standing-wave ratio (*VSWR*) as given by (Milligan, 2005):

$$VSWR = \frac{V_{max}}{V_{min}} = \frac{(1 + |k|)}{(1 - |k|)} \quad (2.10)$$

Where:

V_{max} = the maximum voltage levels of the standing wave.

V_{min} = the minimum voltage levels of the standing wave.

In general, the value of k is a complex quantity, because the terms to be substituted in equation (2.9) are complex quantities. The amount of the power being reflected from a mismatch load is given by $V_i^2|k|^2/Z_0$, whereas the amount of the power being incident is V_i^2/Z_0 and the incident voltage wave is V_i . The factor $|k|^2$ representing the ratio of the returned power to the amount of incident power. Thus, the decibel value of the magnitude of the voltage reflection coefficient is representing the return loss (*RL*) (Milligan, 2005):

$$RL (dB) = -20 \log|k| \quad (2.11)$$

The antenna will be supplied by a certain amount of power, some of this power will be taken by the antenna and other amount of power will be reflected, and this reflected power could be given as:

$$\text{Reflected Power Loss (dB)} = 10 \log(1 - |k|^2) \quad (2.12)$$

The impedance source is the complex conjugate of the antenna impedance that obtains maximum power transfer (Milligan, 2005).

2.1.7. Bandwidth (BW)

The antenna bandwidth is defined as the frequency range over which the antenna is working under certain desired features, according to some conditions and referring to a specified standard (Balanis, 2008). In other words, the bandwidth can be defined as the span of frequencies, oriented around the center frequency, where the antenna characteristics like: (pattern, polarization, beam-width, input impedance, beam direction, radiation efficiency, gain and side lobe level) are within a reasonable range of deviation from those values at the center frequency. Therefore, the absolute bandwidth (*ABW*) of an antenna is given as (Balanis, 2008):

$$ABW = f_U - f_L \quad (2.13)$$

Where f_L and f_U , are the lower and the upper frequency, respectively, which measured at the points of the reflection coefficient curve that crossing the -10 dB level which opposite to $VSWR = 2$, as shown in figure 2.3.

For antennas working on wider range of frequencies (*i.e.* broadband antennas) then the bandwidth is often defined as the ratio of the f_U to f_L for acceptable values of operation, (Balanis, 2008; Stutzman, 1981).

$$BW = \frac{f_U}{f_L} \quad (2.14)$$

But for the narrowband antennas, then fractional bandwidth (*FBW*) is given, as follows:

$$FBW = \frac{f_U - f_L}{f_c} * 100\% \quad (2.15)$$

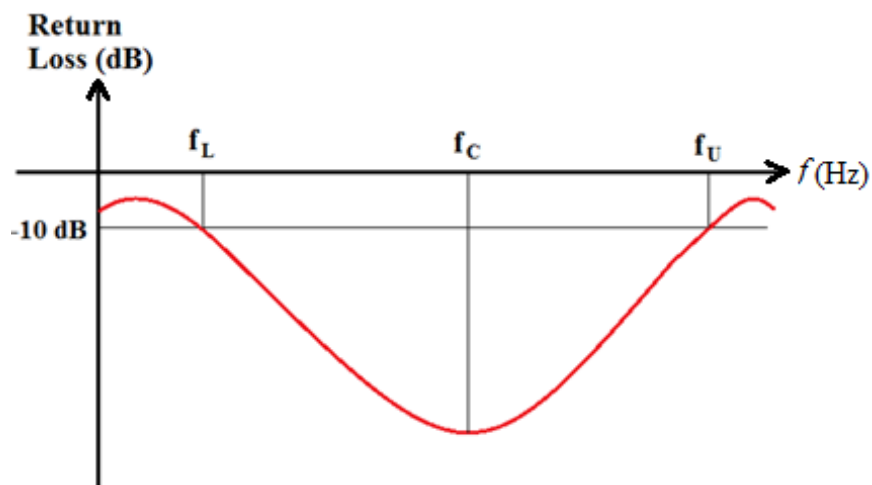


Figure 2.3. Bandwidth measuring from the curve of reflection coefficient.

2.2. Microstrip Antennas

The microstrip radiator was originally proposed for the first time in 1953 by Deschamps (Deschamps, 1953). As depicted in figure 2.4, the simplest configuration of a microstrip antenna be composed of a radiating patch on one side of a dielectric substrate ($\epsilon_r < 10$), which has a ground plane on the other side. The patch connectors, typically gold or copper, can have almost any shape, but normal shapes are usually used to simplify analysis and predict performance. However, the permittivity ϵ_r of the substrate must be small value ($\epsilon_r < 2.5$) to improve fringe fields which measure for radiation. While on other hands, some other performance features may require higher ϵ_r substrate materials. Therefore, different types of substrates have been developed to produce vast range of permittivity and loss tangent amounts. Even some of these materials are flexible in somehow enables fabrication of wearable antennas or wraparound conformal antennas (Garg, 2001).

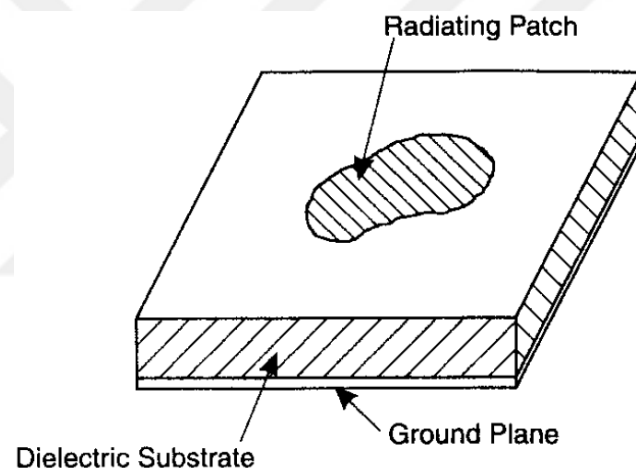


Figure 2.4. Configuration of Microstrip antenna (Garg, 2001).

2.3. Main Types of Miniaturized Antenna

The main challenge in designing any miniaturized antenna is how to make it working on lower frequency band because the lower frequency having longer wavelength which is not easy to be maintained within the dimensions of a small size antenna. But fortunately there are some antennas types having different edge lengths that provide a resonating at multiple frequencies such as; fractal antennas and the slot antennas.

2.3.1 Multiband Fractal Antennas

Fractal geometries have been introduced lately in the design of antennas. Antennas appear in the shape of fractional features related with the geometric characteristics of the diffused fractal. One Feature related with the fractional geometry used in antenna design is self-similar. In this respect a particular shape is repeated and the number of times is scaled to form the final fractional geometry. The repeated shapes can lead to multi-band process (Puente, 1997). The other feature is the capability to collect more electrical length into a given physical size. Therefore, a much reduced antenna can be achieved for the same resonance frequency, which is repeated in a number of frequency bands (Anguera, 2004). One of the main advantages of using fractal geometry is the possibility of new wideband antenna designs with reduced size. The interesting characteristics of fractal antennas that are not found in ordinary antennas promote the application of fractal concepts to more fields of antennas such as being used for miniaturizing antennas while maintaining the multiband operation.

The specifics of the fractal antenna geometry were investigated to figure out their fluent contribution to generate multiband feature (Best 1, 2002; Best 2, 2002). Figure 2.5 shows the first iteration and fourth iteration of the Sierpinski gasket monopole antenna. These antennas having a 15.24 cm as overall height. The practical measurements of return loss for the fourth iteration antenna is shown in figure 2.6 which representing the maximum number of multiband resonance performed by this antenna lying between 50 MHz and 12 GHz. The multiband attitudes of this antenna (the resonant frequencies of congruent minimum VSWR) agree with the consecutive fractal iterations. This reveals that particular specifics of the antenna structure participate to its multiband conduct, and also it could be noticed that within the same triangular shape multi smaller size triangles are maintained without needing for extra extensions, so that the lower frequency accordingly required the larger triangle while the smaller ones are belong to the higher resonating frequencies. As previously mentioned the big problem facing the miniaturization process of the antenna is its lower frequency of operation.

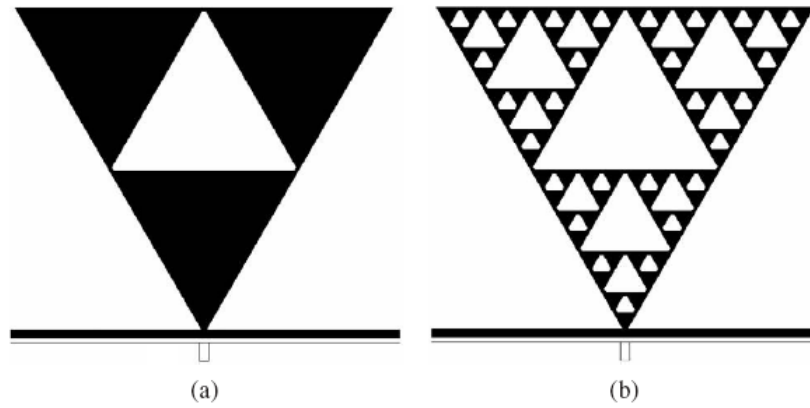


Figure 2.5. Fractal Sierpinski gasket monopole antenna (a) First iteration (b) Fourth iteration (Puente, 1997; Anguera, 2004).

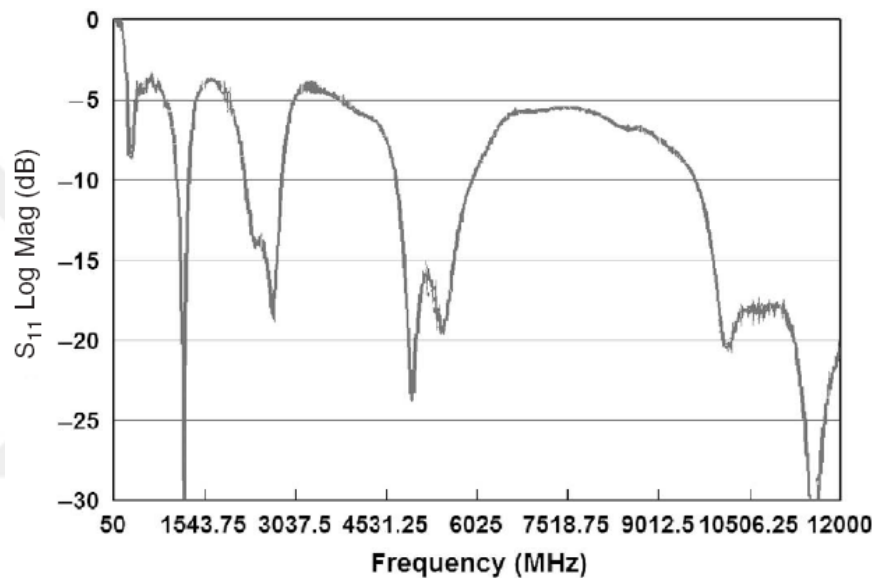


Figure 2.6. The Sierpinski gasket measured return loss with fourth iteration over a frequency range of (50 MHz to 12 GHz) (Best₁, 2002; Best₂, 2002).

2.3.2. Slot Antennas

Slot antennas (SA) are one of the common omnidirectional antennas, which characterized by their radiation patterns that being omnidirectional azimuthally and their polarization is horizontal. The waveguide slot antennas (WSA) consisting of array of slots are usually used for higher gain that can be designed at frequencies from 2 to 24 GHz, as shown in figure 2.7.a, while simple slotted-cylinder antennas are more common at the Ultra High Frequency (UHF) and lower frequencies of microwave as shown in figure 2.7.b where the size of a waveguide becomes unwieldy (Paul Wade, 2001). As an enhanced version of the slotted-cylinder antenna, the Alford slot is designed with higher gain compared to the previous one.

The typical example of SA is formed by making a rectangular slot cut in an extended thin flat sheet of metal with the free slot to permit radiation on both sides of this sheet, as shown in figure 2.8. Then the excitation of this slot is established by a voltage source such as a coaxial transmission line or a balanced parallel transmission line that being connected to the opposite edges.

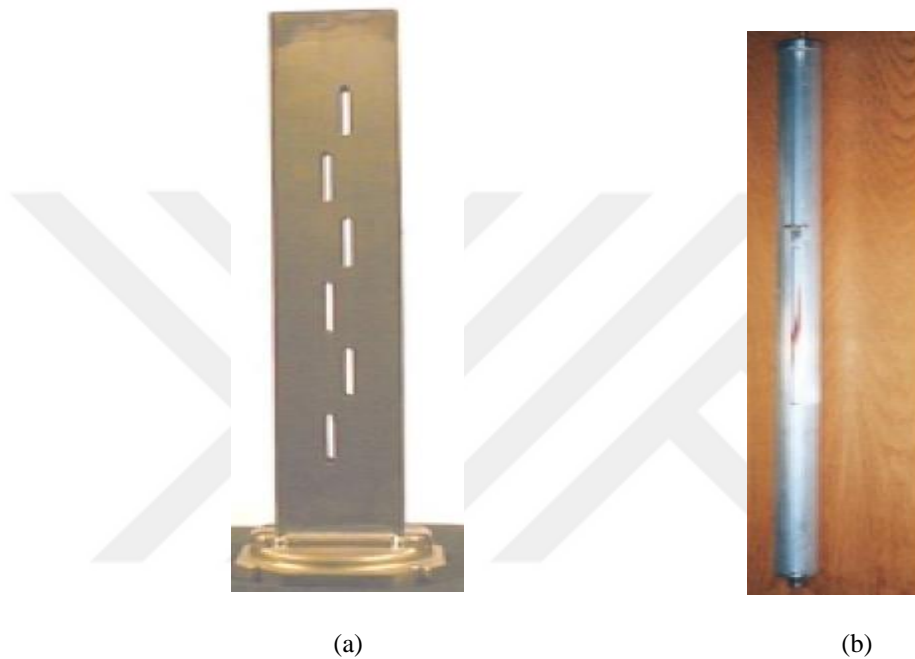


Figure 2.7. (a) Waveguide slot antenna. (b) Simple slotted-cylinder antenna (Paul Wade, 2001).

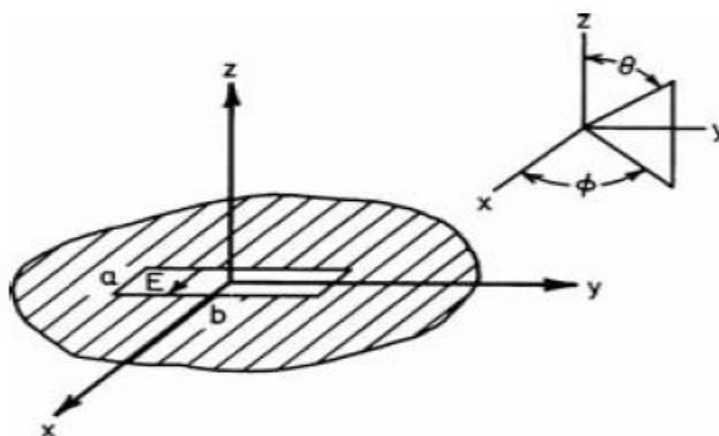


Figure 2.8. Rectangular slot (John, 2007).

In the slot the electric field distribution can be getting from the relationship between the slot antennas and complementary wire. It has been shown that the distribution of the electrical field (or the magnetic current) within the slot is corresponding to the distribution of electrical current on the complementary wire. For the rectangular slot illustrated in figure 2.8, the electric field is normal to the longitudinal edge and its magnitude will get zero value at the ends due to being tangential with the narrow edges.

The electrical field intensity is normal to the surface of the slot antenna everywhere, in exception of the zone of the slot itself.

The theoretical background of this antenna shows that the radiation due to the flow of currents in the sheet can be derived directly from the electric field distribution within the slot. Thus, the field radiation of an elementary magnetic moment inside the boundaries of the slot should comprise the contribution offered by the flowing of the electric current on the metal surface.

Often the slot antennas design requires cutting the slot in somehow unlike a dilated flat sheet surface. Whatever be the surface, the electric field will be normal all over the surface except the region of the slot. The field radiated from the electric currents on this metal surface can be derived from the magnetic currents exciting the slot, similar to the flat metal sheet case. The combination of the aforementioned field along with the exciting field will result in the total field resulted from the magnetic currents on the given boundary surface. Therefore if a thin rectangular slot with certain area is cut into a circular cylinder, then the electric current distribution will differ from other case if these slots have been added to a flat metal sheet.

Generally, the slot antennas are not radiating on both sides of that surface including them because either one side is totally enclosed (e.g., the slotted cylinder antenna), or it is desired to minimize the radiation on one side which enables the antenna to be directional antenna. In these cases, the effect of the enclosed cavity region on the excitation and impedance of these slot antennas has a great importance on the design of the antenna (John, 2007).

The important think concerning to the miniaturization process of antennas is the relation between the inner edges of the slot antenna and the wavelength of the resonating frequency, so that if smaller size is required then it needs to maintain that wavelength within small slot, which may be achieved by using corrugated edges.

2.4 Radio-Frequency Identification (RFID) Antennas (Application Example)

Antennas are the starting and ending points of the channels for the transfer of data between the reader and the tag. Antenna design and placement plays an important role in determining the scope, accuracy, and coverage area of communication (Sanghera, 2011; Bhuptani, 2005). Commonly the tag antenna is fabricated with the tag chip on the same packaged and surface as one single component; figure 2.9 shown that the antenna configurations and some common passive tag. Since the tag chip can be very small, less than 1 millimeter square, the dimension of packaging for the entire tag usually determined by the shape and size of the antenna. The packaging features of the reader antenna also vary according to the requirements of the application. In some cases such as handheld readers, the antenna is directly manufactured on the reader. In other cases, multiple antennas can be installed away from the reader and put them strategically to enhance the quality and scope of radio signals (Sanghera, 2007; Bhuptani, 2005).

Another nowadays example is the smart watch which is being designed by many manufacturers competing in compacting its size with all of inside circuitry and the very high integrated components. The antenna of smart watch is built inside its belt for maintaining small size and not needing for extra extensions as shown in figure 2.10 (Zhao, 2015).

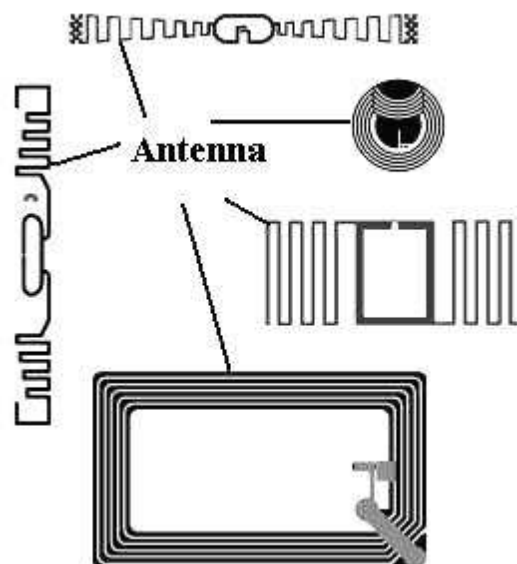
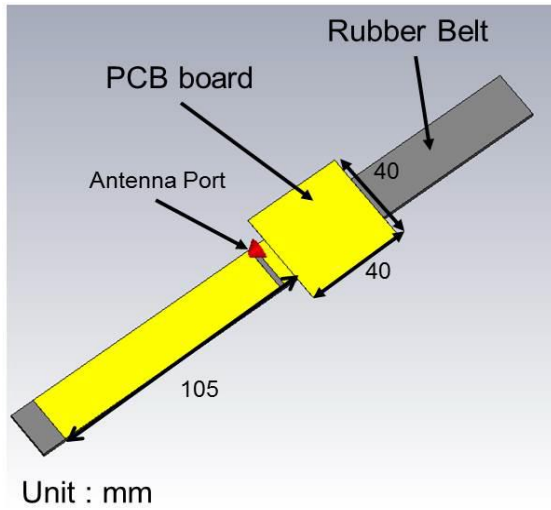
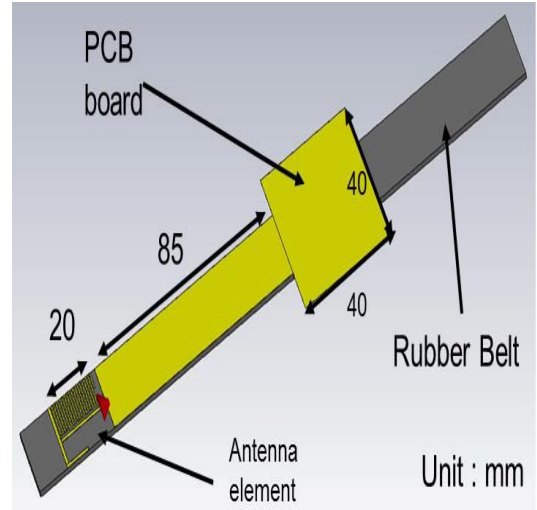


Figure 2.9. A typical passive RFID tags with antenna.



(a)



(b)

Figure 2.10. Smart watch Antenna Structures of (a) Dipole antenna (b) Monopole antenna (Zhao, 2015).



3. MATERIAL AND METHODS

3.1. Material

The requirements for this research are vary between surveying literatures for inspiring new designs, simulating the designed antennas and validation through fabrication and practical measurements. In general they could be listed as follows:

1. Sufficient literatures to start the investigation are already available. More surveys will be needed.
2. Software package to deal with the analysis of the problem by computer simulations has been acquired recently which is CST Microwave Studio 2014 as shown in figure 3.1.

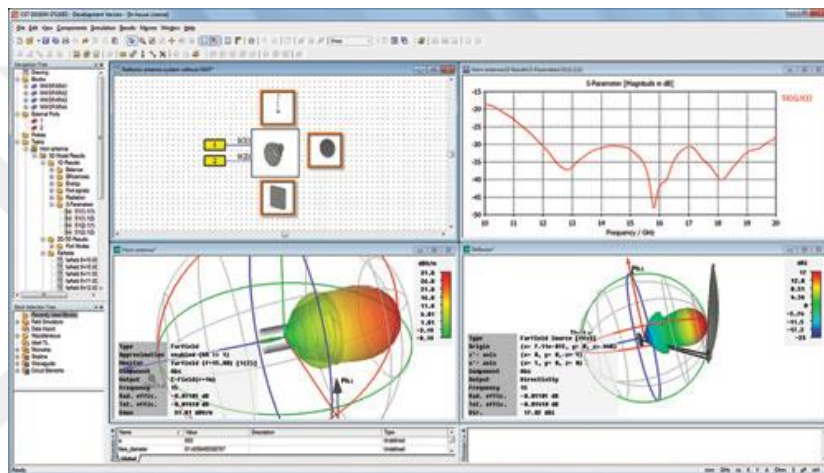


Figure 3.1. Overview of CST Microwave Studio 2014 Software Package.

3. Some of the required experimental facilities are already available in the Department of Electrical and Computer Engineering / UoD, such as the FR4 copper PCB boards for implementing the planar microstrip antennas as shown in figure 3.2.



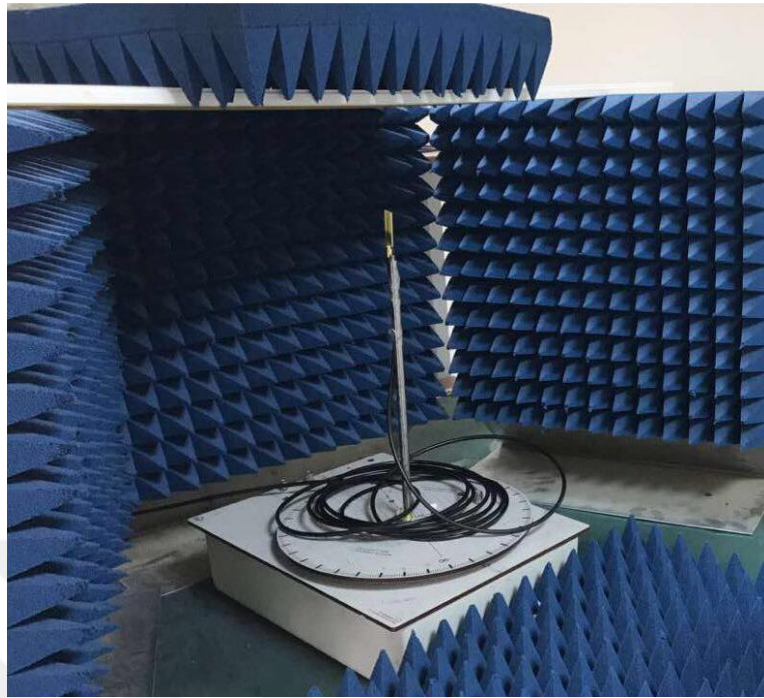
Figure 3.2. FR4 copper PCB boards.

Also a Rohde & Schwarz[®] ZVL13 (VNA) ranged from (9 kHz ~ 13.6 GHz) is available as shown in figure 3.3.

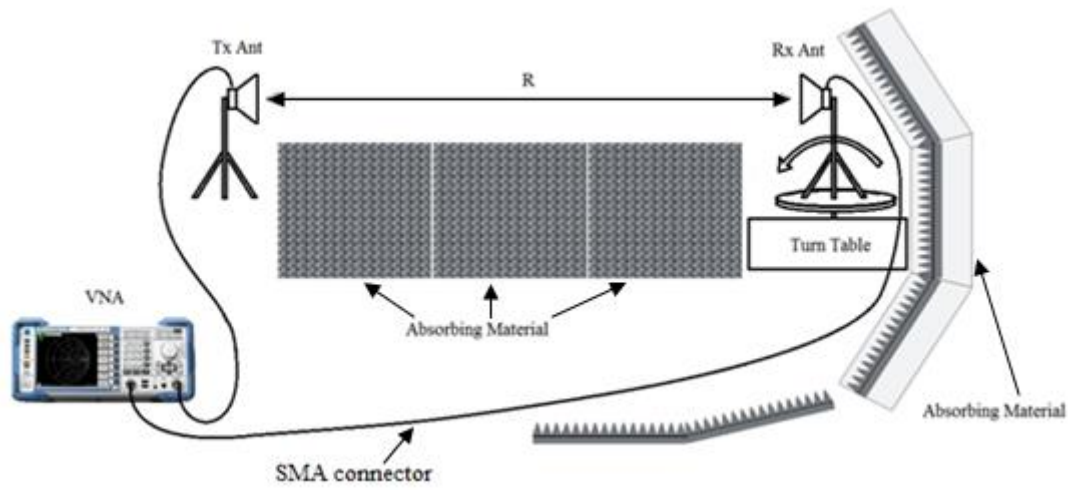


Figure 3.3. The Vector Network Analyzer Rohde & Schwarz[®] ZVL13 with frequency range of (9 kHz ~ 13.6 GHz).

The existence of VNA is useful in the measurement of the return loss (S_{11} or S_{22}) for the designed antennas, and also it helps performing the radiation pattern measurements by fixing the transmitting antenna (Tx Ant) and rotating the receiving antenna (Rx Ant). Each of these antennas must be connected to one of the two ports of VNA then measurements for S_{12} or S_{21} will be taken. The measurement either of these two aforementioned S-parameters will be considered as the received power to be normalized or plotted to generate the radiation pattern for the Rx Ant. The measurement setup is shown in figure 3.4.



(a)



(b)

Figure 3.4. The Measurement Setup, (a) Perspective view, (b) Layout view.

4. MATLAB R2015a has been used for plotting the measured data and comparing with the simulation one.

3.2. Methods

3.2.1. Miniaturization of a Planar Strip-Shaped Monopole Antenna (PSSMA) for WLAN Application

Recently the a very large scale integration has been performed in wireless communication devices in such a manner that enables compacting them within small packages or even tags while working on single or multiple frequency bands. The microwave components required by these systems need for miniaturization day by day as much as developments are achieved, especially that the trend is to make these devices smaller in size while maintaining their high performance almost unchanged.

Among the challenges to design such devices is the design of their antennas which desired to be compacting within their packaging. The design of such antennas required making the physical length of their edges and aspects equal to the effective electrical length required for resonating at certain frequencies. The desired frequencies are essentially allocated for the wireless applications according to international standards.

Microstrip antennas have been commonly used in nowadays military and commercial communication applications, due to their planar structure, small size, low cost, easily fabricated and acceptable performance. Therefore, the microstrip boards are hardly nominated for introducing miniaturized antennas and many attempts are suggested to reduce the size of microstrip antennas such as using Defected Microstrip Structure (DMS), Defected Ground Structure (DGS), high permittivity dielectric substrate at the ground plane or combination of them (Chakraborty, 2012; Hanae, 2015). antennas require several of the communication systems be working at multiband ranges of frequencies, and this has been attained by dissimilar methods like using of slots, fractal method, notch technique and metamaterial (Alam, 2012; Sayem, 2006). Others replaced the normal ordinary substrates by a μ -negative metamaterials (MNG) which miniaturize the rectangular patch antenna size to 77% (Bazrkar, 2012).

The meandering technique for the microstrip feed line has been used in previous work to conduct impedance matching over a very wideband range of frequencies. This technique was proposed to modify UWB antennas being designed using certain formulas (Fadhel, 2011; Sayidmarie, 2012). Other researcher has corrugated the edges of the ground plane and radiator of a planar Tapered Slot Antenna (TSA) to reduce its overall size while maintaining its properties without changing (Abbosh, 2009).

A planar square monopole antenna has been introduced by (Ahirwar, 2010) to cover the frequency range of (300 to 3000 MHz). Then modification has been added by corrugating its square radiating element laterally. In spite of reduction in the width of its radiating element has been performed with about 60% but its height wasn't changed, and also after modification the antenna has not remained planar anymore. Where as in the section after the next one, the corrugation and meandering techniques have been employed to miniaturize the whole size of a simple PSSMA while maintaining the other features and planarity of the parent strip-shaped antenna unaffected

3.2.1.1. Antenna Design

A PSSMA antenna has been designed as a simple planar monopole antenna that works on 2.45 GHz to serve in WLAN devices. The PSSMA is an extension from the microstrip feed line as shown in figure 3.5. The antenna structure has been designed according to (Ray, 2008) as follows:

$$f_L = \frac{c}{\lambda} = \frac{7.2}{(L + r + P) * k} \text{ GH} \quad (3.1)$$

Where r is the values of the radius and L is the value of height of a virtual cylindrical monopole antenna, in that order. This is the virtual equivalent of the antenna as a PSSMA antenna. According to this method proposed in (Ray, 2008), it can be calculated as follows:

$$L = L_{rad} \quad (3.2)$$

$$r = \frac{W_T}{2\pi} \quad (3.3)$$

Where the value of the strip-shaped radiator length is L_{rad} , the microstrip feed line width value is called W_T , and P is the length in cm of the 50 Ω feed line between the radiator and the ground plane, however in this design the radiator is an extension of to the microstrip feeding line by having the same width, so P will be included in the L_{rad} dimension or omitted, and value of $k = \sqrt{\epsilon_{eff}}$. The value of ϵ_{eff} is approximated given by (Balanis, 2005):

$$\epsilon_{eff} \approx \frac{\epsilon_r + 1}{2} \quad (3.4)$$

Having a thickness for FR4 substrate is taken as 1.6 mm, accordingly equation (3.4) gives k to be 1.627, and $\epsilon_{eff} = 2.65$. This value is suggested by (Matin, 2011) to be taken

as the value of experimental 1.15. So the value of $L_{rad} = 25.4$ mm, if the lower frequency is chosen to be 2.45 GHz, but will be taken (25.5 mm) instead of (24.5 mm).

The length of the ground plane has been taken as a quarter of the effective wave length $L_G = (\lambda_{eff}/4)$, and $\lambda_{eff} = c/\sqrt{\epsilon_r}f$. The value of ϵ_r is 4.3 for FR4 substrate, and the frequency for WLAN has been taken 2.45 GHz, then $L_G = 14.5$ mm and $\lambda_{eff} = 58.4$ mm.

The microstrip width is feed line and named W_T has been determined according to below (Wadell, 1991; Wheeler, 1977):

$$Z_o = \frac{87}{\sqrt{\epsilon_r + 1.41}} \ln \left(\frac{5.98 h}{0.8 W_{StrL} + t} \right) \quad (3.5)$$

Where Z_o is the microstrip feed line feature impedance, h is the thickness of substrate which has been taken as a typical value 1.6 mm, t is taken as 0.035 mm which is the metallization thickness, W_{StrL} is the microstrip feed line width, and ϵ_r is 4.3 for FR4 substrate. Therefore, W_{StrL} must be equal to 3 mm for a characteristic impedance of 50 Ω , and for simplicity W_{StrL} has been named W_T in figure.3.5. All of the above-mentioned parameters of design along with other values are shown in the Table 3.1.

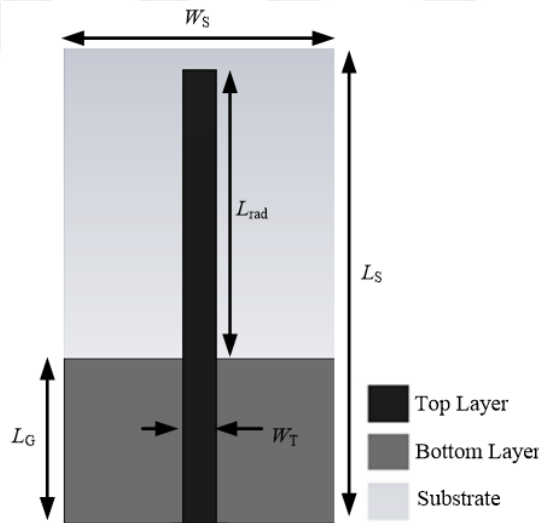


Figure 3.5. Geometry of the simulated PSSMA.

Table 3.1. Design parameter of PSSMA.

Parameter	Dimension (mm)
L_{rad}	25.5
L_S	42
L_G	14.5
W_S	24
W_T	3

3.2.1.2. Miniaturization

After the PSSMA antenna has been designed, it is necessary to miniaturize it while preserving its features. The miniaturization has been executed by two unlike methods. Firstly, by corrugating the strip-shape radiator edges in somehow to get repeating slots along the edges.

The corrugated PSSMA antenna is shown in figure 3.6. These slots have been optimized by simulation to get optimized values for the length (L_{Slot}) and depth (W_{Slot}) as shown in Table 3.2. It has been shown that this technique reduces the real physical height of the radiator but the electrical path necessary to the flow of the current has been almost kept unchanged, because the current flowing through the radiator will essentially distributed at the edges and it will follow a corrugated path in its flow to get the desired path length, while the overall size is reduced to 89.3% ($37.5*24/42*24=0.8928$) of the original antenna.

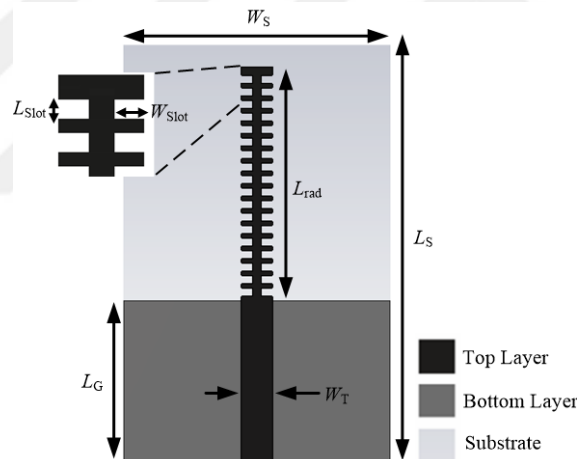


Figure 3.6. Geometry of the simulated corrugated PSSMA.

Table 3.2. Design parameter of corrugated PSSMA.

Parameter	Dimension (mm)
L_{rad}	21
L_{Slot}	0.75
L_S	37.5
L_G	14.5
W_S	24
W_{Slot}	1
W_T	3

The second technique suggested for miniaturizing of PSSMA has been performed by the meandering the strip-shaped radiator to minimize the overall height of the radiator while keeping the actual path desired against the current. However the overall height has been decreased physically while maintaining the electrical length desired to keep the resonating in the same frequency of the original antenna.

The meandered PSSMA antenna is shown in figure 3.7 and Table 3.3 listed all of its parameters. This antenna dimensions have been optimized to get closer characteristics to the parent antenna, and the overall size is reduced to 85.7% ($36 \times 24 / 42 \times 24 = 0.857$) of the original antenna.

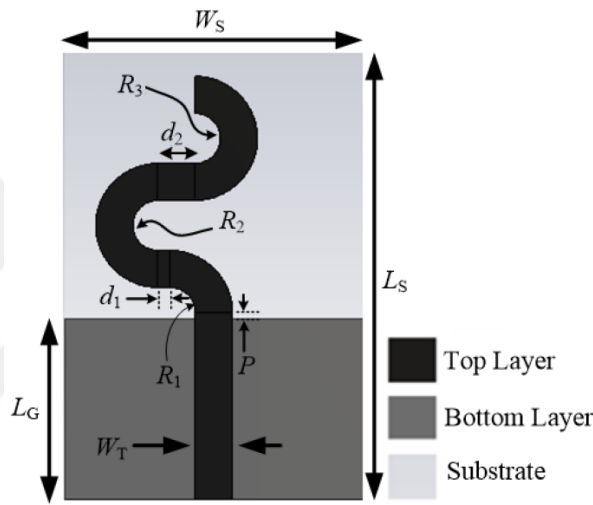


Figure 3.7. Geometry of the simulated meandered PSSMA.

Table 3.3. Design parameter of meandered PSSMA.

Parameter	Dimension (mm)
d_1	1
d_2	3
R_1	2
R_2	2
R_3	2
L_s	36
L_G	14.5
P	0.5
W_s	24
W_T	3

3.2.2. Miniaturization of a Planar Circular Monopole Antenna (PCMA) For UWB Application

Since adopting the UWB standard by Federal Communication Commission (FCC) in 2002 (Federal Communications Commission, 2002) for short-range peer-to-peer ultra-fast communication, researchers competed in designing different types of antennas that obey the wideband range of frequencies (3.1 GHz ~ 10.6 GHz) which is required by this technology. Some of these antennas were planar and others were non-planar. Concerning to the planar microstrip antennas the main challenge was represented in its narrow band features, which has been overcome via designing a certain shapes of antennas that having different aspect lengths in front of the exciting current to be resonating with different wavelengths which in turn widening the range of frequencies to cover the UWB range. Among these shapes were; the triangular, elliptical, circular, ring, etc. (Sayidmarie, 2011; Sayidmarie, 2012). It has been concluded in (Fadhel, 2013) as a common silent characteristic between all of these designed antennas shapes that; the impedance bandwidths of these antennas will be wider as much as the edges of their radiating elements are having a round or curved shapes. In turn, this will be more convenient of their features with UWB requirements.

In spite of the complexity in designing of these UWB antennas but the challenges were raised up when different techniques suggested for miniaturizing them. For instance, symmetrical exponential corrugations have been introduced in the radiator of tapered slot antenna (TSA) by (Bead'a, 2014) which enables the antenna to resonate at lower frequencies with comparably smaller size structure. The depth of these corrugation slots has been selected to be less than quarter of the effective wavelength at the lowest operation frequency, and this represents an inductive reactance to the passing wave which in turn increases the effective electrical length of the structure. Although the TSA antenna in general, is characterized by its directional radiation pattern, but omnidirectional TSA has also been introduced as that in (Bialkowski, 2011), where some corrugations have been made to miniaturize its size. In addition to these aforementioned benefits of corrugations in miniaturization of planar antennas, it has been shown in (Chareonsiri, 2017) that adding the corrugation slots could improve the antenna gain very efficiently, where several corrugation shapes like; rectangular, sawtooth and cosine shapes were used. Therefore, corrugation technique has been used in this thesis to modify the circular radiator of PCMA which given 42.6% of reduction compared to the original antenna size.

Other technique of miniaturization depends on the current distribution analysis to suggest elimination for some metalized areas of that antenna, like that performed in (Chen, 2013), in which a crescent-shape has been introduced as a miniaturized shape of original elliptical shape radiator. Another work by (Azenui, 2007) evolved the crescent-shape antenna from elliptical shape by carving a circular hole inside the radiator symmetrically, which succeeded to remove 40% of the metallization and 60% of the ellipse area. But these aforementioned works have failed to make reduction in the overall size. Unlike other design in (Nikolaou, 2016) which modified a slot antenna that enabled up to 63% of miniaturization after removing some areas but the modification here was associated with major changes in the shape of the antenna by changing the U-shape radiator to cactus shape, and also the modified antenna has not stay slot antenna anymore .

The elimination of undesired areas is introduced in this thesis due to aforementioned reasons but with minor changes in the shape of the original antenna, in a trial to enhance the design procedure that might be generalized to other shapes of planar antennas. The miniaturization process suggested here is considered as a complementary process for the main design procedure. The original antenna to be designed will be a PCMA as one of the common UWB antennas, and its current distribution will be simulated, to figure out the undesired or least current distributed areas. Then these areas will be eliminated to generate the planar crescent-shape monopole antenna (PCSMA) which will achieve a reduction in size by not less than 11.8% while almost maintaining the same characteristics as that of the original antenna.

3.2.2.1. Antenna Design

A PCMA antenna has been designed as a simple planar monopole antenna to be working on the entire UWB frequency range. The PCMA antenna is an extension from the microstrip feed line as shown in figure 3.8. The antenna volume has been designed according to (Ray, 2008) as follows:

$$f_L = \frac{c}{\lambda} = \frac{7.2}{(L + R + P) * k} \text{ GHz} \quad (3.6)$$

Where L and R are the values of the effective height and radius of a virtual cylindrical monopole antenna, respectively. This virtual antenna considered as an equivalent for the PCMA antenna. Due to this method have been calculated as follow: (Ray, 2008),

$$L = 2A \quad (3.7)$$

$$R = A/4 \quad (3.8)$$

Where R is the radius of the circular radiator, P is the neck length in cm of the 50 Ω microstrip feed line between the radiator element and the ground plane, the width of the microstrip feed line is W_T , but in this design the radiator considered as an extension to the microstrip feed line by having the same width, so value of $k = \sqrt{\epsilon_{eff}}$ and P will be omitted or included in the L_C dimension. The ϵ_{eff} approximated value has been notified in equation (3.4)

The thickness value is 1.6 mm if FR4 substrate has been used, the values of $\epsilon_{eff} = 2.65$, and accordingly k is 1.627 which has been given from equation (3.4). This value is suggested by (Matin, 2011) to be taken 1.15 as empirical value. Therefore if the lower frequency is chosen to be 2.45 GHz, then $L_C = 12$ mm.

The ground plane length has been taken as a quarter of the effective wavelength $L_G = (\lambda_{eff}/4)$, and $\lambda_{eff} = c/\sqrt{\epsilon_r}f$. The value of ϵ_r is 4.3 for FR4 substrate and for WLAN the frequency has been taken as 2.45 GHz, then ($\lambda_{eff}=58.4$ mm) and $L_G = 22.7$ mm.

The microstrip feed line width W_T has been calculated in equation (3.5) and for simplicity W_{StrL} has been called W_T in figure 3.8. The PCMA design parameters shown in the Table 3.4.

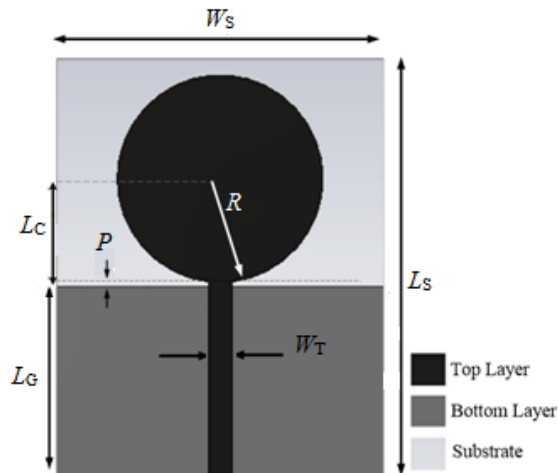


Figure 3.8. Geometry of the simulated PCMA.

Table 3.4. Design parameter of PCMA.

Parameter	Dimension (mm)
P	0.5
R	12.5
W_s	40
W_t	2.8
L_s	51
L_g	22.7
L_c	13

3.2.2.2. Miniaturization

After designing the PCMA antenna, it is necessary to miniaturize it while preserving its features almost unchanged. The miniaturization process has been implemented by two dissimilar methods. The first technique was achieved through eliminating the areas with least distributed surface current which generates a crescent-shaped radiator to decrease the overall height of the radiator while maintaining the same desired real path against the current.

So the overall height has been reduced physically while the desired electrical length has been preserved to conserve resonating at the same frequencies as that of the original antenna. Figure 3.9 shown the PCSMA antenna and Table 3.5 shown the all of its parameters. The PCSMA antenna dimensions have been improved to obtain closer characteristics to the parent antenna, and reducing the total size to 88.2% ($40 \times 45 / 40 \times 51 = 0.882$) of the original antenna.

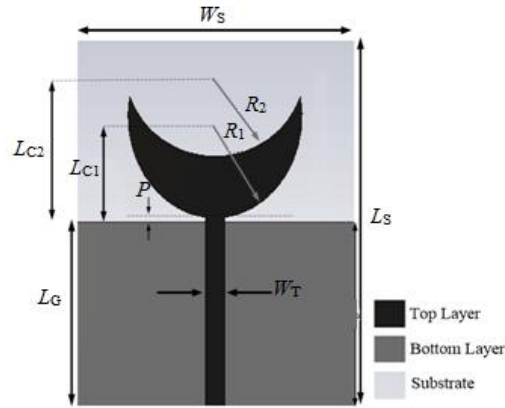


Figure 3.9. Geometry of the simulated PCSMA.

Table 3.5. Design parameter of PCSMA.

Parameter	Dimension (mm)
L_{C1}	13
L_{C2}	19
L_S	45
L_G	22.75
W_S	40
W_T	2.8
P	0.5
R_1	12.5
R_2	11

The second technique of miniaturization the PCMA antenna is performed by corrugating the circular radiator edges in somehow to get repeated slots around its round edge. The size of these slots have been improved to obtain optimum length (L_{Slot}) and depth (W_{Slot}) as shown in figure 3.10 and all of its parameters are shown in Table 3.6. This technique has reduced the original physical height of the radiator but the electrical path required for the current has remained virtually unaffected, because of the current flowing within the radiator will essentially distributed at the edges and it will follow a corrugated path to get the desired path length just like the original PCMA but with least size. Accordingly, the antenna important characteristics have been preserved while the overall size is reduced to 57.4% ($30 \times 39 / 40 \times 51 = 57.35\%$) of the original antenna.

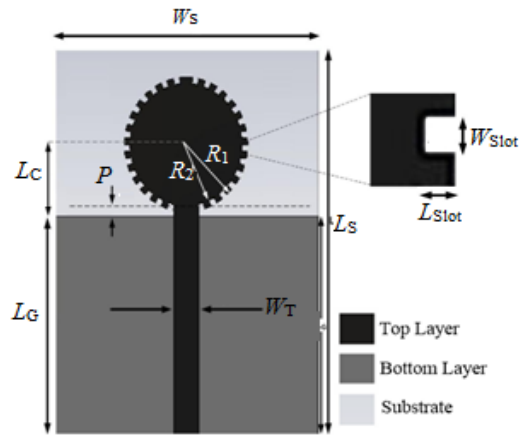


Figure 3.10. Geometry of the simulated corrugated PCMA.

Table 3.6. Design parameter of corrugated PCMA.

Parameter	Dimension (mm)
L_C	7.65
L_{Slot}	0.65
L_S	39
L_G	22.75
W_S	30
W_{Slot}	1
W_T	2.8
P	0.5
R_1	7
R_2	6.35

4. RESULTS AND DISCUSSION

4.1. Miniaturization of a Planar Strip-Shaped Monopole Antenna (PSSMA) for WLAN Application

The PSSMA has been designed as mentioned in chapter three, then two techniques have been used to miniaturize it; corrugating and meandering. All designed antennas have been simulated by using CST Microwave Studio 2014. Figure 4.1 depicted the simulation results of the return loss curves versus frequency for the planar PSSMA, corrugated PSSMA, and meandered PSSMA. It shows that all these antennas maintain their work on the band 2.45GHz for WLAN while the meandered PSSMA advanced in getting another resonant band suitable for 5.5 GHz as well. Investigating the surface current distributions for the three designed antennas are shown in figures 4.2 to 4.4, it has been shown that the surface current is almost concentrated at the radiators edges. So in corrugated PSSMA the current follows the corrugated path of the radiator edge and it will cross the in demand path with lower height compared to the straight PSSMA, which achieves this method of miniaturization. In the meandered PSSMA the same thing happened as well, but this time it has been done via meandering the whole strip-shaped radiator to get more reduction in the overall height and more forcing of the current to follow a zigzag or meandrous way. The meandering technique is became a dual-band WLAN planar antenna instead of single-band because fortunately at higher frequency band of WLAN, this technique has gained another resonating around 5.5 GHz.

After completing the simulation and design antennas of the above mentioned, fabrication of all three antennas have been done as described in figures 4.5 to 4.7, and examined via Rohde & Schwarz[®] ZVL13 VNA. The measured and simulated return loss data for all three antennas and as shown in figures 4.8 to 4.10. The measured and simulated data almost agree with each other, except some deviations due to some shortages in the manufacturing, especially that of shifting of the lower resonating dip. However, the practical measurements validate the design and the modification and adjust its work to minimize the overall size of the PSSMA. Therefore the antennas which were miniaturized will be working with most similar characteristics with least size which was the aim of this research.

The simulated and measured radiation patterns in H and E planes for the three antennas are shown in figures 4.11 to 4.13. Measured radiation patterns are almost meet

the simulated patterns. And also shown that the radiation patterns have not been affected by the miniaturization process implemented by corrugation nor meandering. The radiation pattern of the meandered PSSMA has been plotted at 5.5 GHz and 2.45 GHz because it works on dual-bands of WLAN. Finally, the simulated realized gain of PSSMA has been calculated to be (1.8 dB) at 2.45 GHz, while it is (1.48 dB and 1.53 dB) at 2.45 GHz for each of the corrugated PSSMA and meandered PSSMA, respectively. These values are moderate values and very comparable to the gain of half wave dipole antenna (*i.e.* 2.15 dB). Also for the meandered PSSMA it was found to be (3.54 dB) at 5.5 GHz. The Comparison of simulated realized gain curves versus frequency for the all three antennas is shown in figure 4.14.

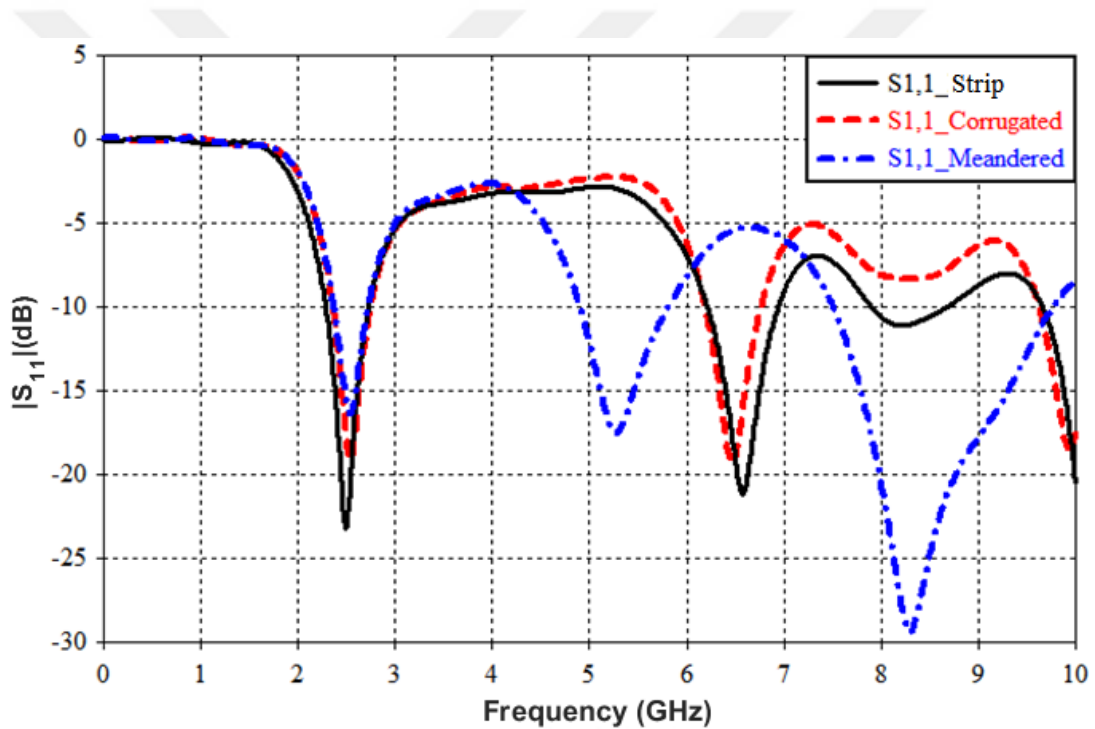


Figure 4.1. Comparison of simulated return loss curves for the PSSMA, corrugated PSSMA, and meandered PSSMA.

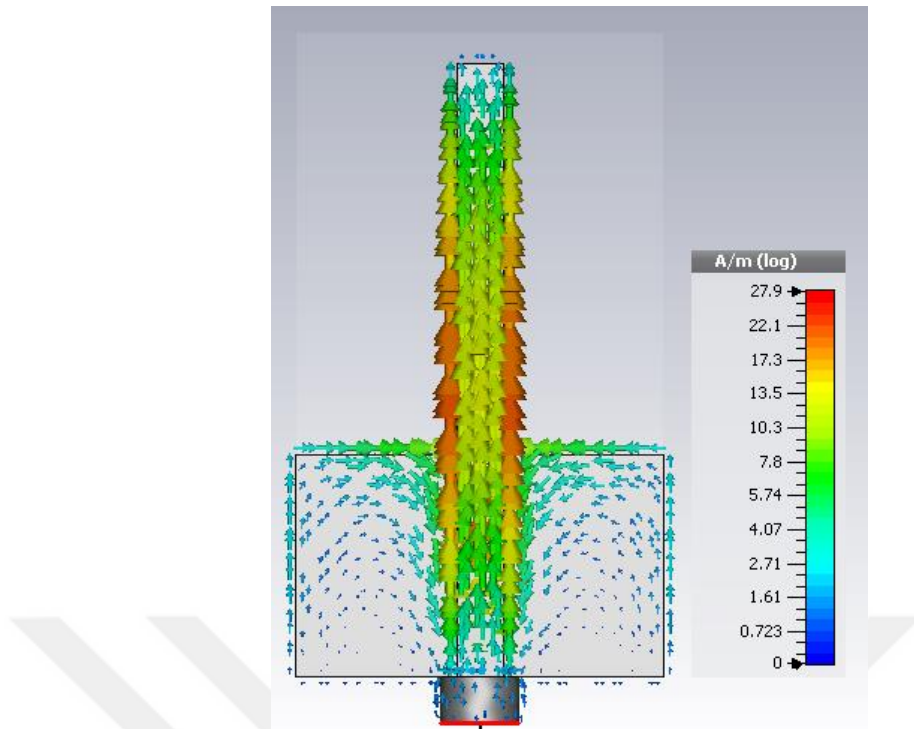


Figure 4.2 PSSMA surface current distribution at 2.45 GHz.

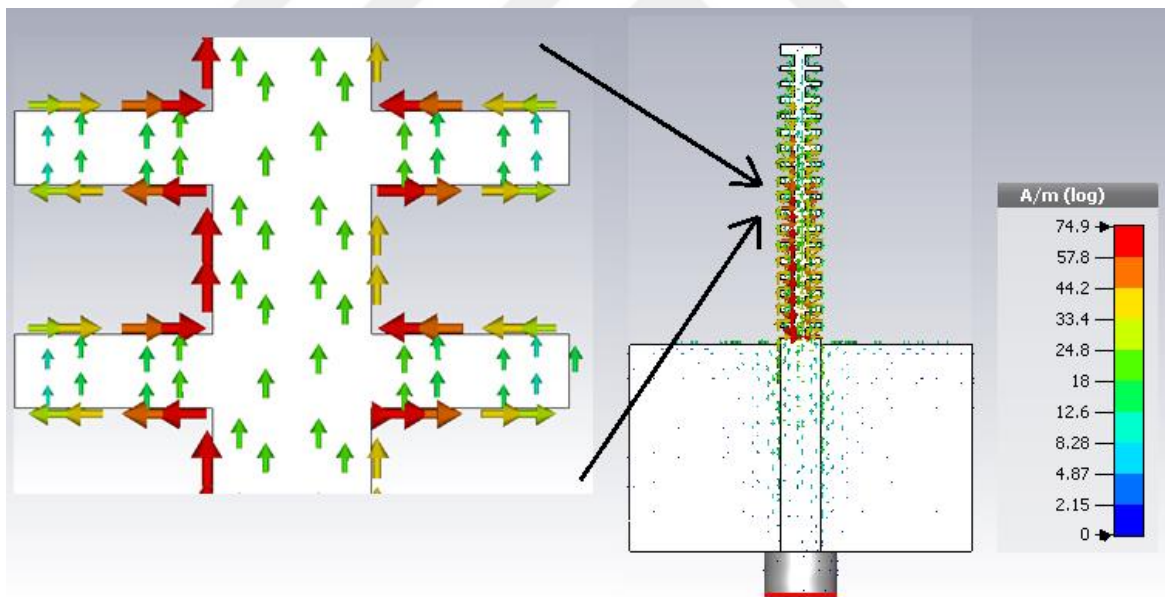
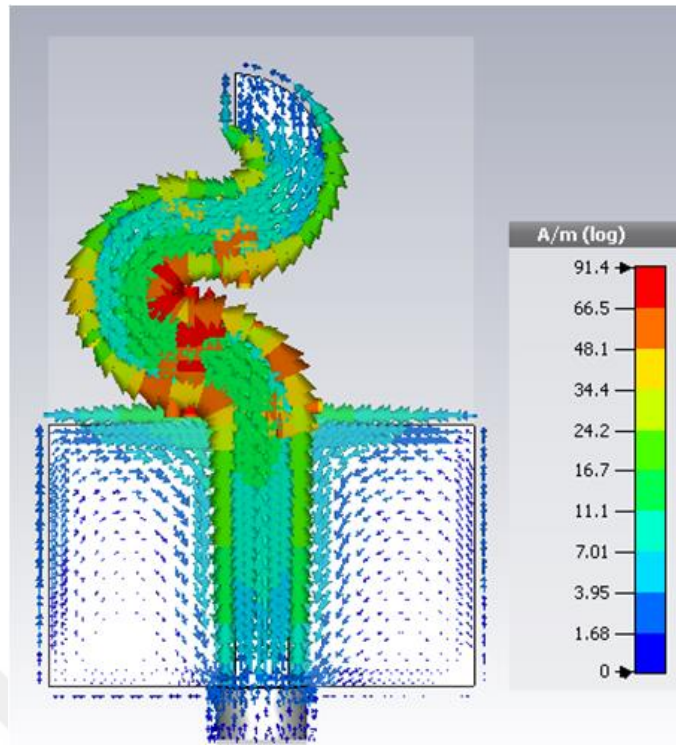
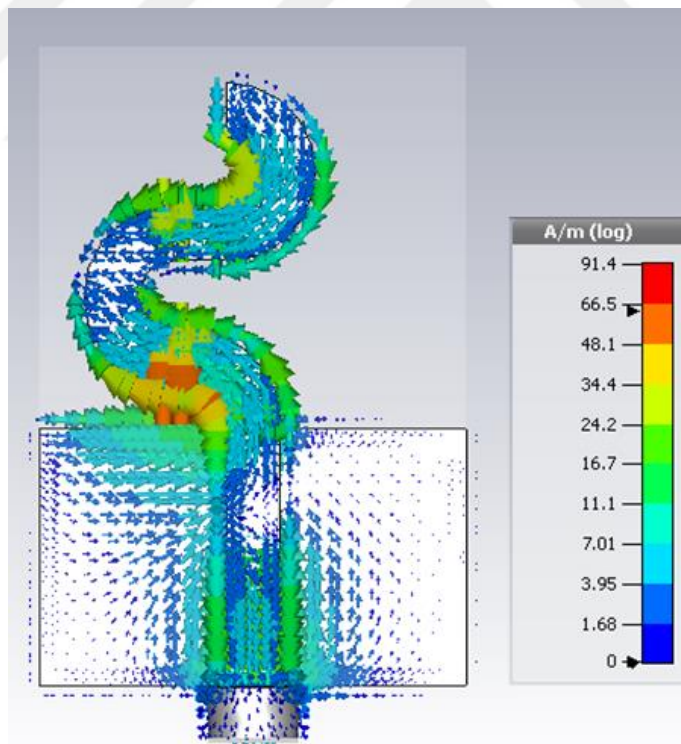


Figure 4.3. Corrugated PSSMA surface current distribution at 2.45 GHz.



(a)



(b)

Figure 4.4. Meandered PSSMA surface current distribution at (a) 2.45 GHz, and (b) 5.5 GHz.

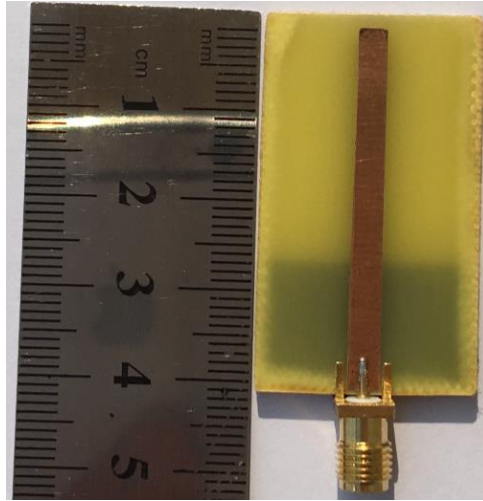


Figure 4.5. Fabricated PSSMA.

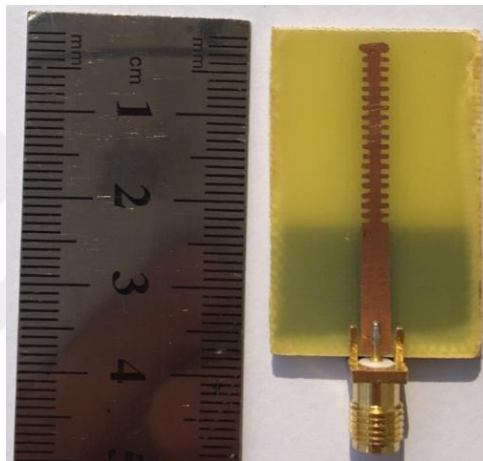


Figure 4.6. Fabricated corrugated PSSMA.

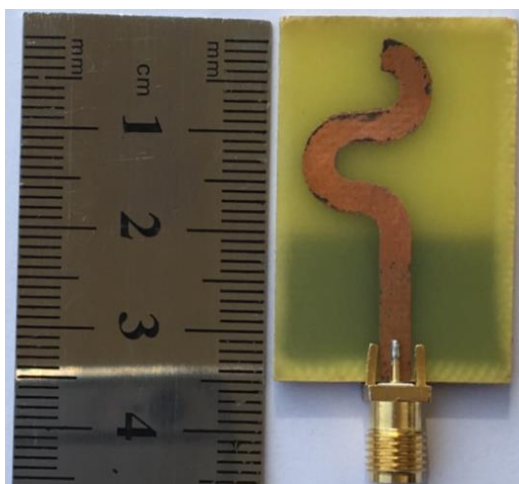


Figure 4.7. Fabricated meandered PSSMA.

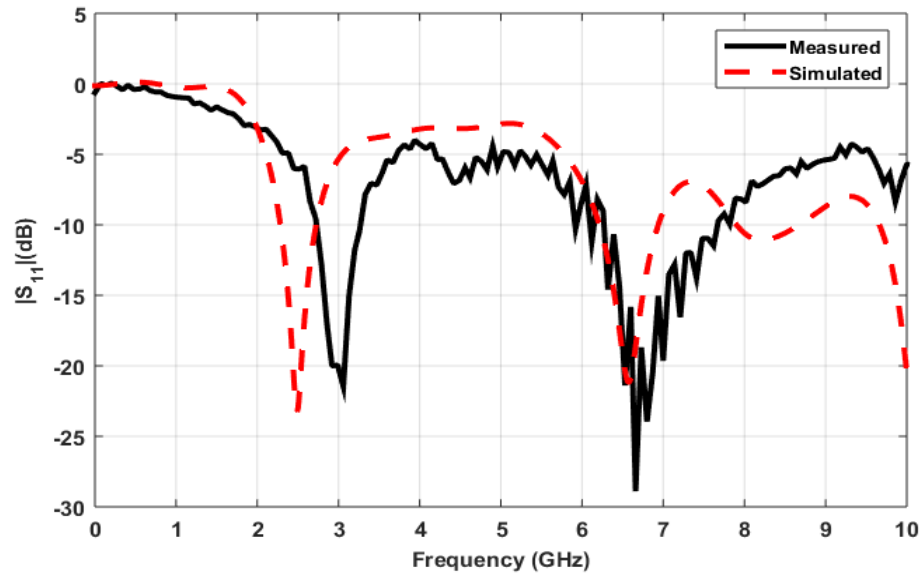


Figure 4.8. Simulated and measured curves of return loss for the PSSMA.

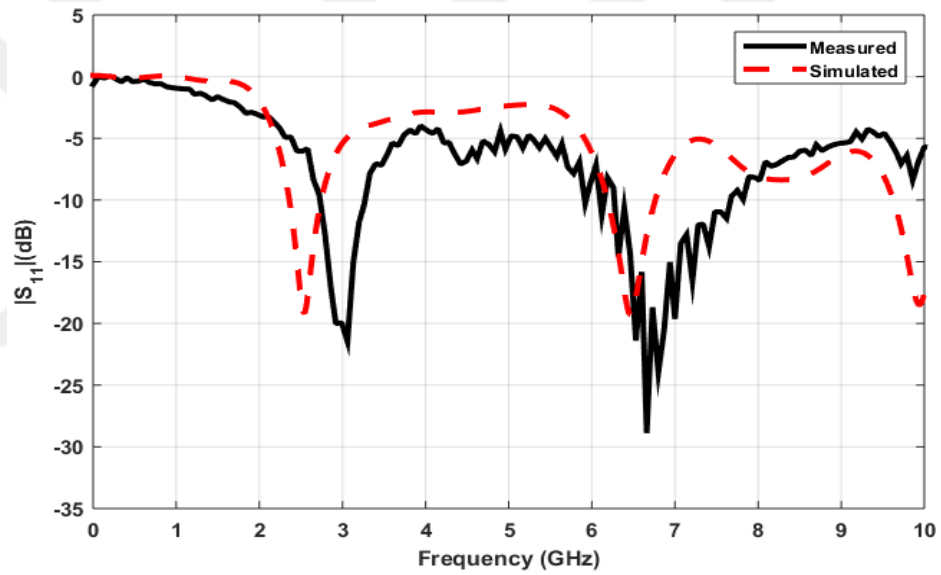


Figure 4.9. Simulated and measured curves of return loss for the corrugated PSSMA.

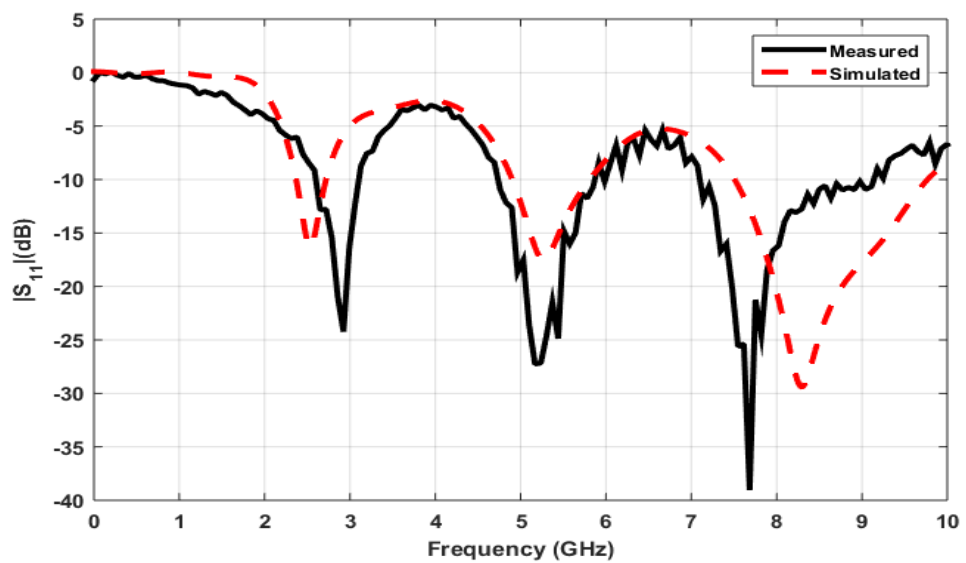


Figure 4.10. Simulated and measured curves of return loss for the meandered PSSMA.

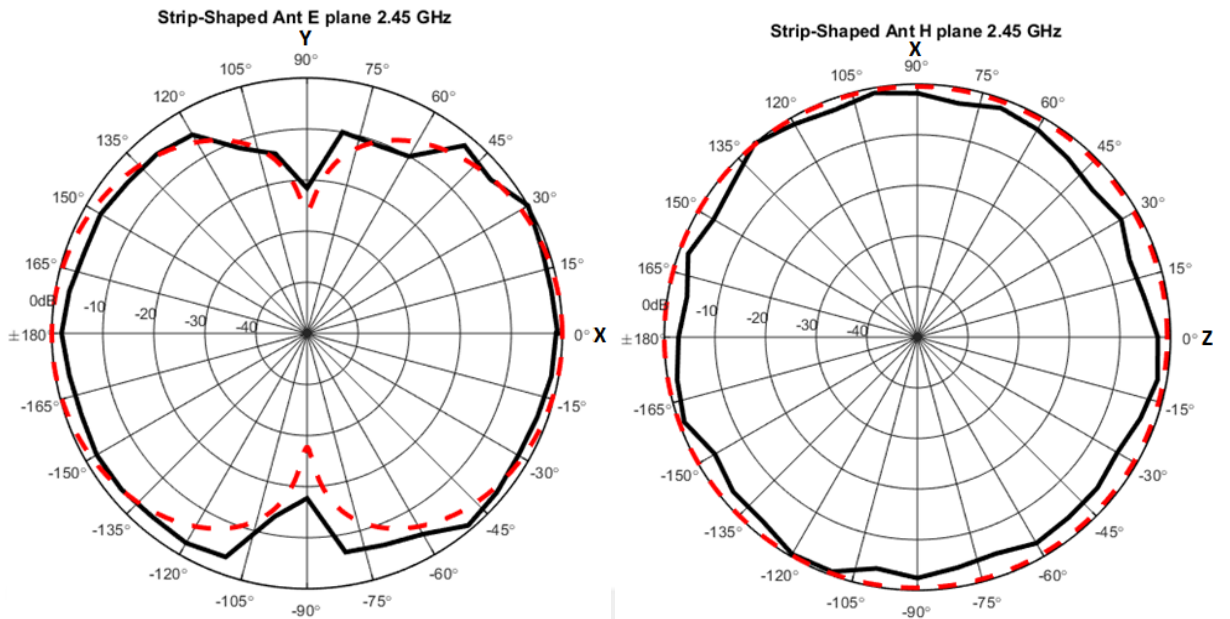


Figure 4.11. Radiation patterns measured (—) and simulated (---) of the PSSMA in E and H planes, at frequency of 2.45 GHz.

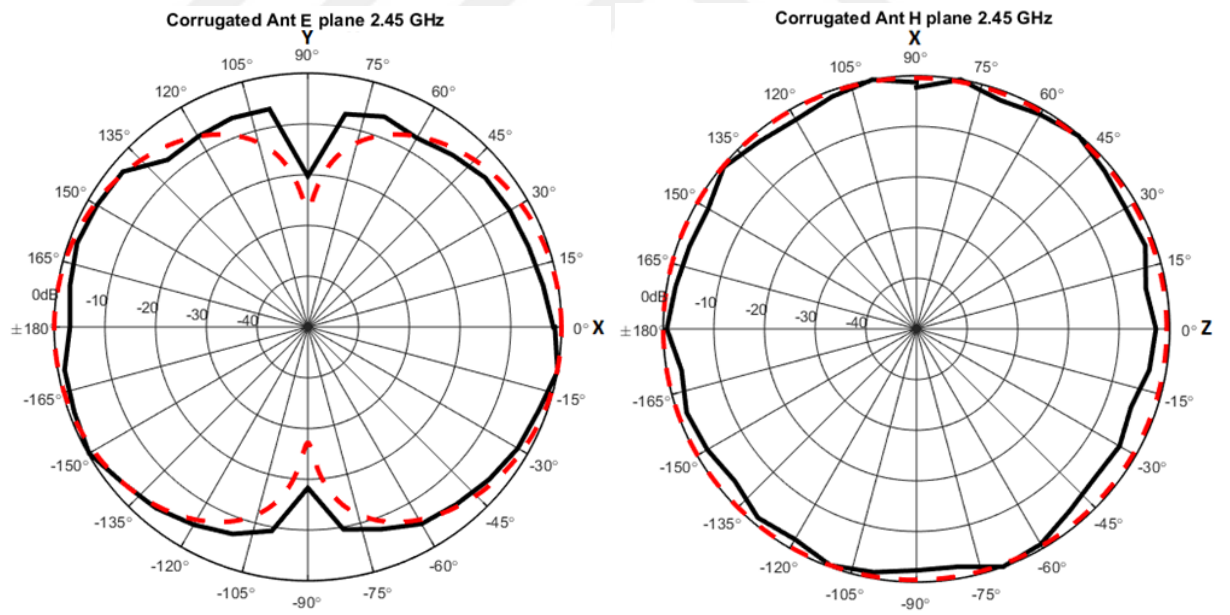


Figure 4.12. Radiation patterns measured (—) and simulated (---) of the corrugated PSSMA in E and H planes, at frequency of 2.45 GHz.

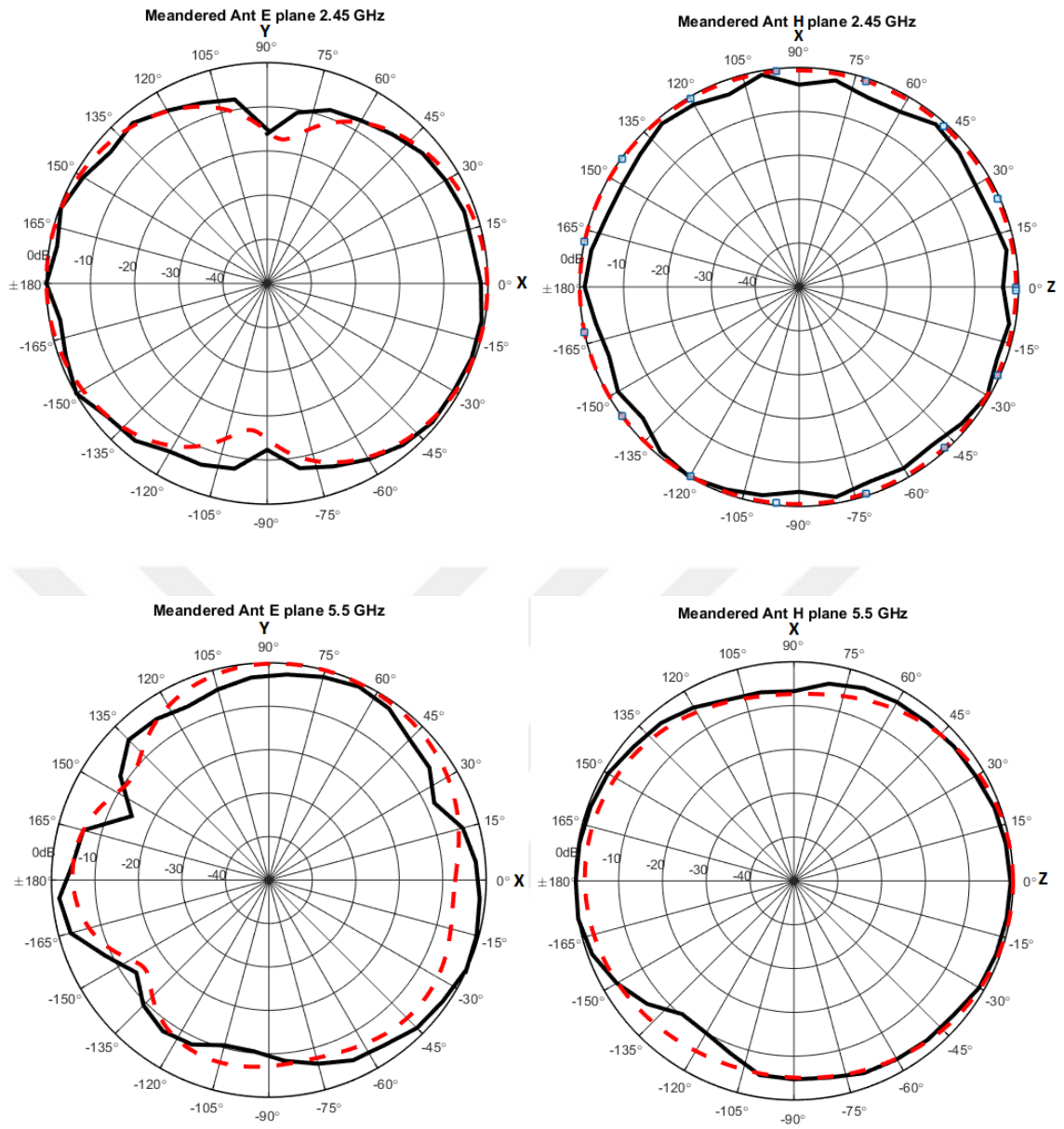


Figure 4.13. Radiation patterns measured (—) and simulated (---) of the meandered PSSMA in E and H planes, at the two frequencies 2.45 and 5.5 GHz.

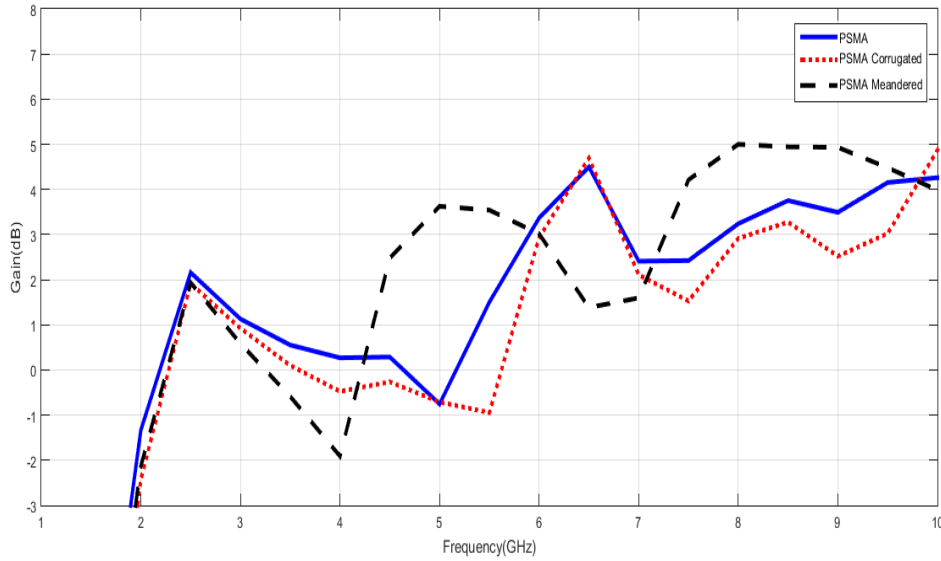


Figure 4.14. Comparison of simulated realized gain curves for the PSSMA, corrugated PSSMA and meandered PSSMA.

4.2. Miniaturization of a Planar Circular Monopole Antenna (PCMA) for UWB Application

PCMA has been designed as one of a very common UWB antenna with dimensions and geometry as mentioned in chapter three, then two different techniques have been used; firstly, by eliminating the undesired or least current distributed areas to generate a planar crescent-shaped monopole antenna (PCSMA), secondly by corrugating the round edge of the circular radiator to miniaturize its circumference. All the designed UWB antennas have been simulated. Figure 4.15 shows the simulation results of the return loss curves versus frequency for the PCMA, PCSMA, and Corrugated PCMA. It shows that all of these designed antennas are maintaining their working which covered the entire UWB. Investigating the surface current distributions for the three designed antennas are shown in figures 4.16 to 4.18 and they were plotted for 5 and 9 GHz of frequencies. The PCSMA will offer the required area of metallization in least size compared to the PCMA. Therefore, it has been concluded that the current will be concentrated at this miniaturized area which is almost distributed at the lower side edges of the radiator. While in corrugated PCMA the current will follow a corrugated path offered by the radiator edge and it will cross the desired path with least height compared to PCMA, which validates this technique of miniaturization.

After completing the design and simulation of antennas that above-mentioned, the all three antennas have been implemented as shown in figures 4.19 to 4.21, and

tested via Rohde & Schwarz® ZVL13 VNA. The return loss data has been measured for the all three UWB antennas and plotted in comparison with their simulation one as shown in figures 4.22 to 4.24. The measurement results is almost agreed with the simulation results except of some deviations like shifting of the lower resonating dip due to some imperfection in the fabrication process. However, the practical experimental measurements validate the design and its modification which performed to miniaturize the size of the PCMA. Therefore the miniaturized antennas will be working with almost the same features with least size which satisfy the goals of this research.

The simulated and measured radiation patterns in E and H planes for the three antennas are shown in figures 4.25 to 4.27 for 5 and 9 GHz of frequencies. Measured radiation patterns are almost meet simulation patterns. And also the miniaturization has nearly not affected the radiation pattern that performed by crescent nor corrugation. Finally, the simulated realized gain curves for PCMA, PCSMA and corrugated PCMA have been plotted as shown in figure 4.28. For PCMA it is noticed that almost the gain is increased with increments in the frequency, which is common in UWB antennas, while for corrugated PCMA and in spite of the great miniaturization occurred in its size but its gain (not less than 2 dB) was still has a reasonable value comparable to the gain of half wave dipole antenna (*i.e.* 2.15 dB), and getting up to (4.8 dB at 9.5 GHz). Although the miniaturization ratio in corrugated PCMA is greater than that of PCSMA but its gain still better than the gain of PCSMA, because in the corrugated PCMA the circumference length is maintained via corrugated edge, while it is truncated in PCSMA.

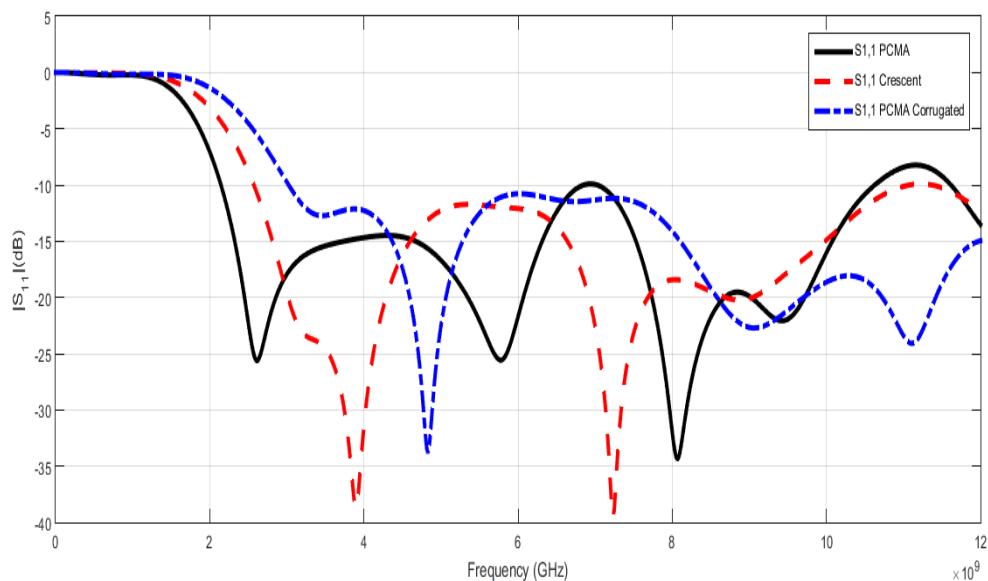
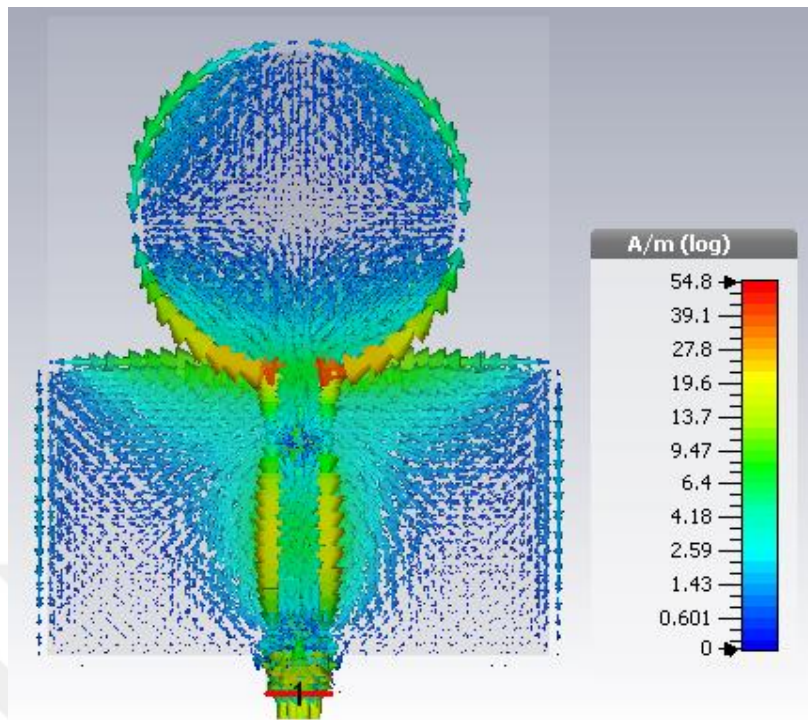
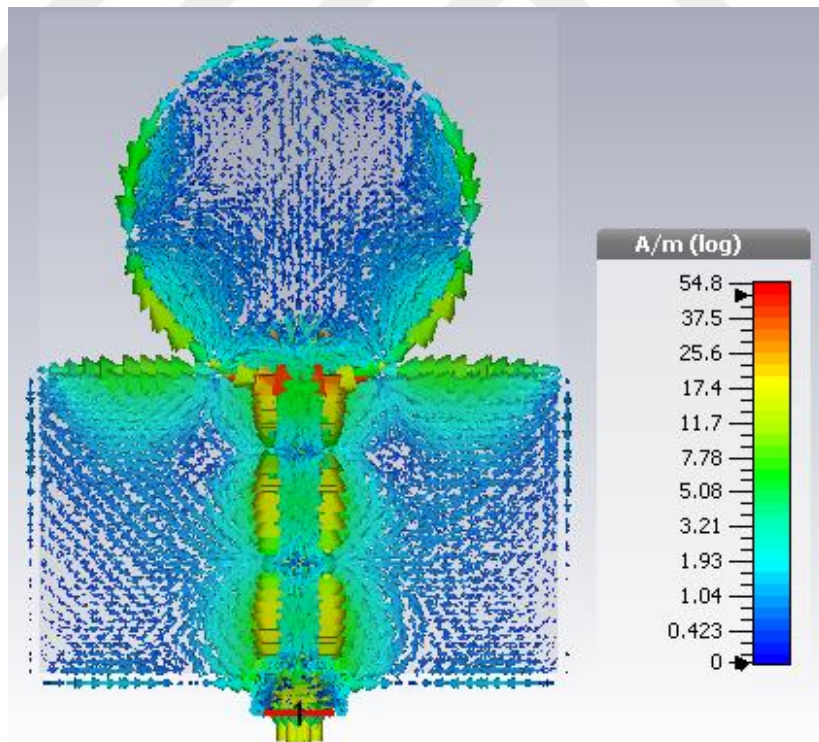


Figure 4.15. Comparison of simulated return loss curves for the PCMA, PCSMA and corrugated PCMA.

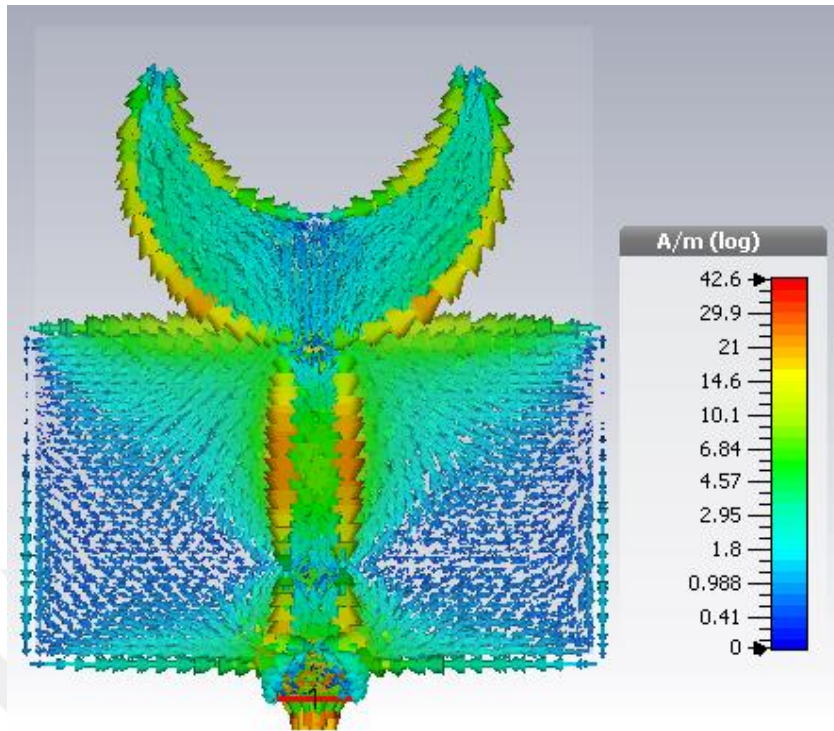


(a)

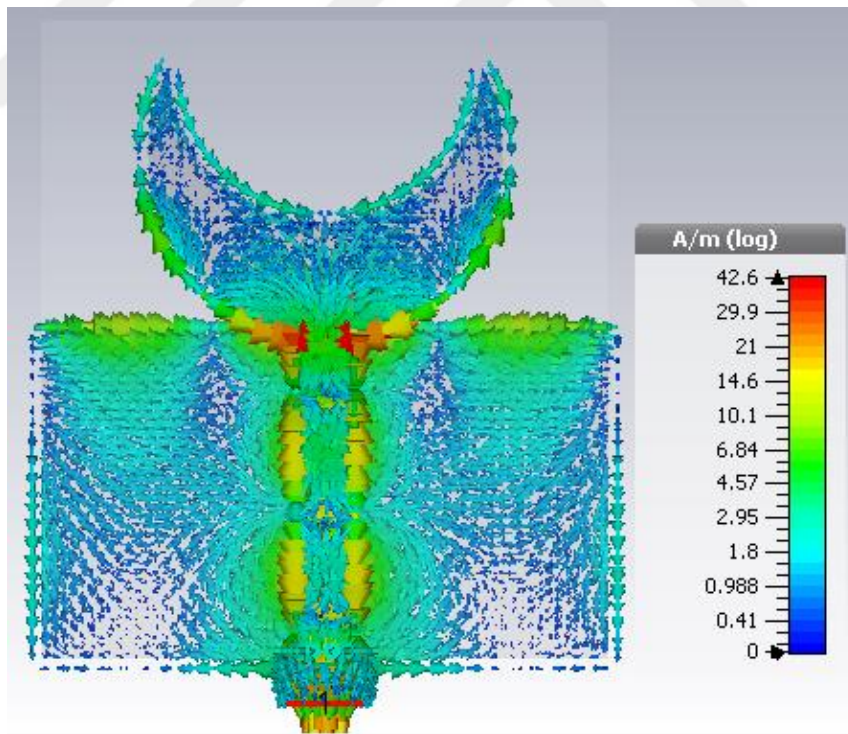


(b)

Figure 4.16. PCMA surface current distribution at (a) 5 GHz, and (b) 9 GHz.

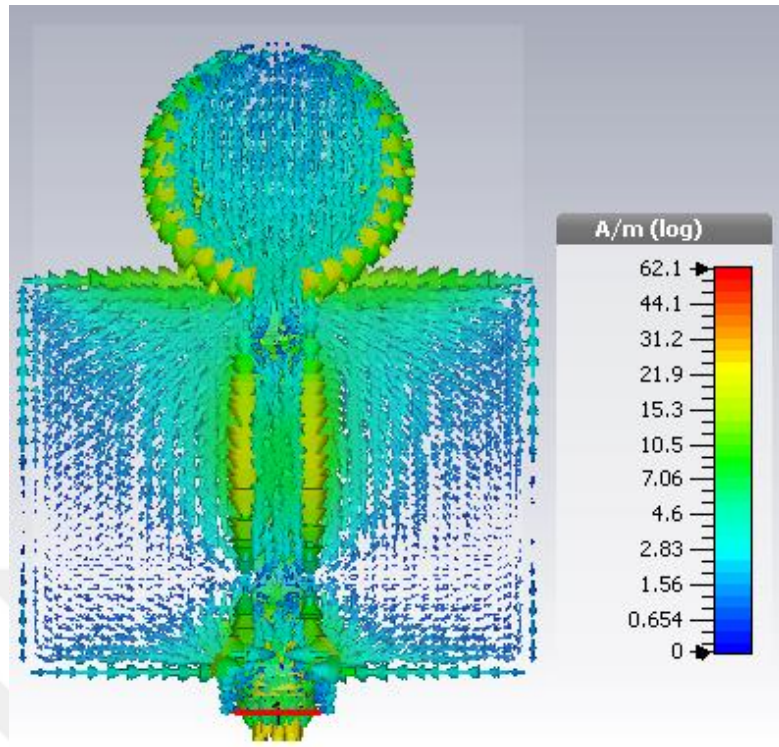


(a)

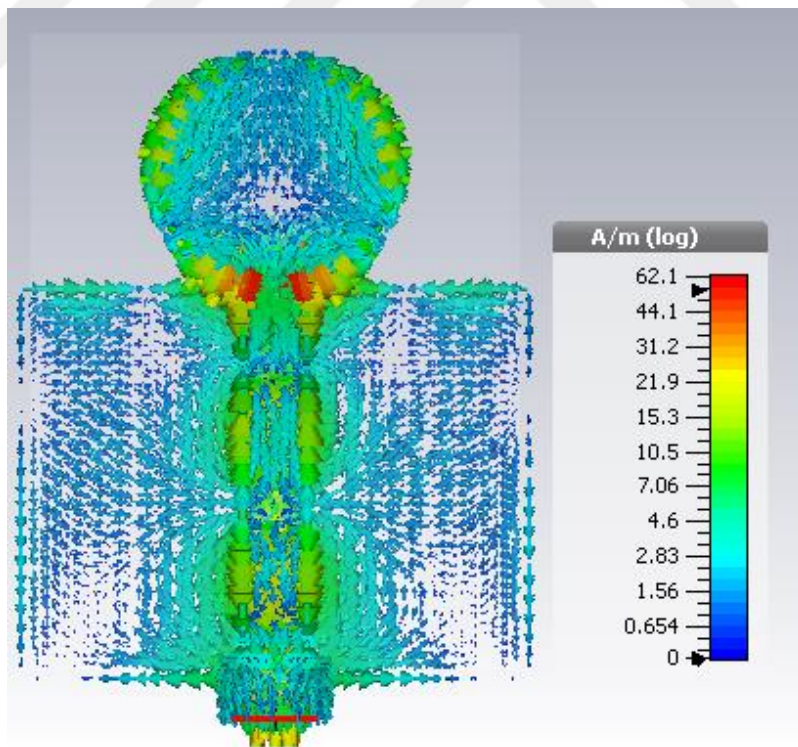


(b)

Figure 4.17. PCSMA surface current distribution at (a) 5 GHz, and (b) 9 GHz.



(a)



(b)

Figure 4.18. Corrugated PCMA surface current distribution at (a) 5 GHz, and (b) 9 GHz.

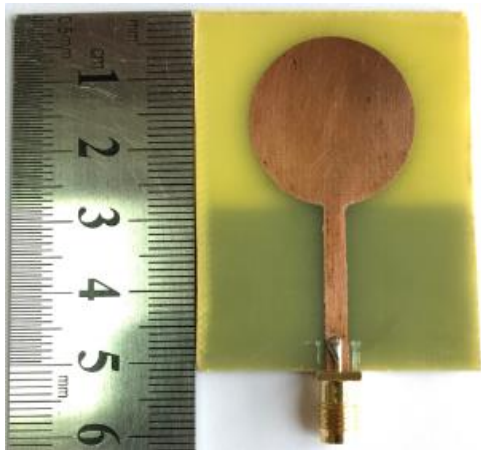


Figure 4.19. Fabricated PCMA.



Figure 4.20. Fabricated PCSMA.

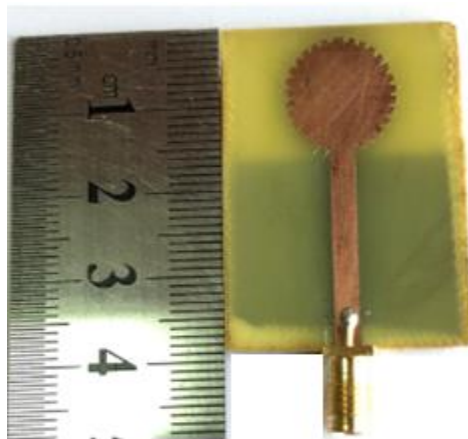


Figure 4.21. Fabricated corrugated PCMA.

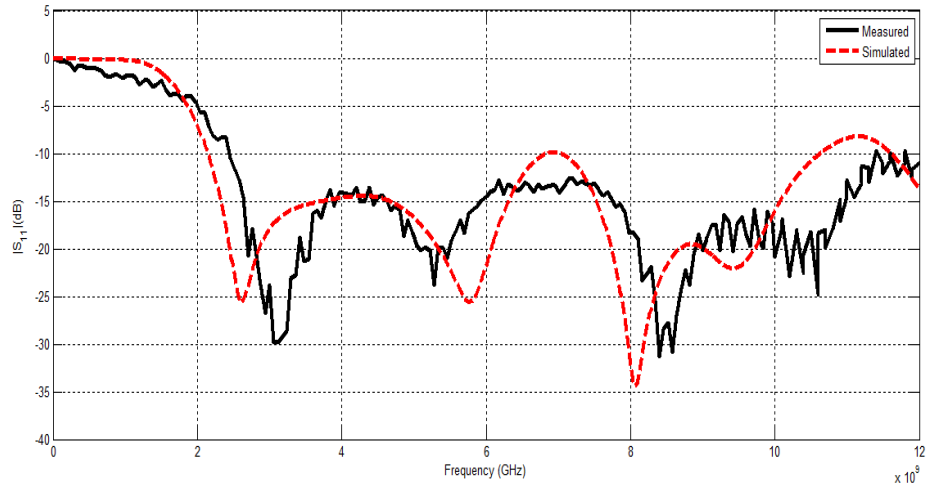


Figure 4.22. Simulated and measured curves of return loss for the PCMA.

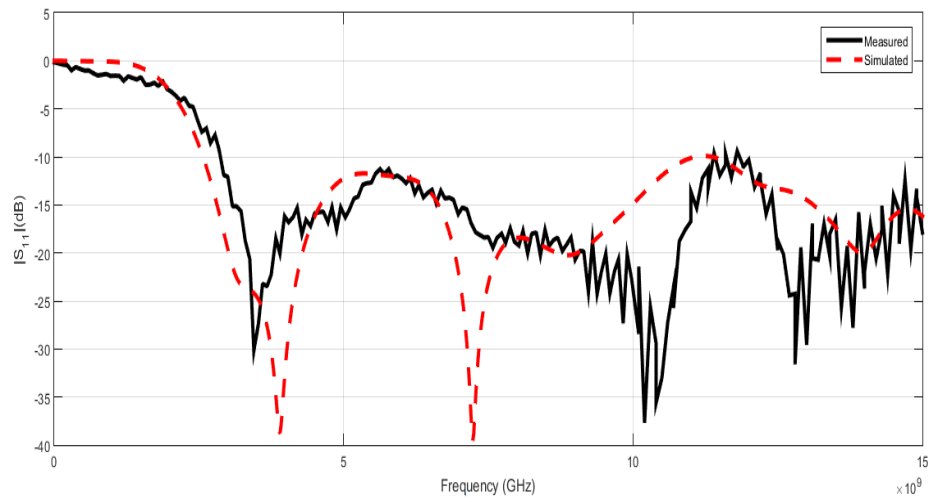


Figure 4.23. Simulated and measured curves of return loss for the PCSMA.

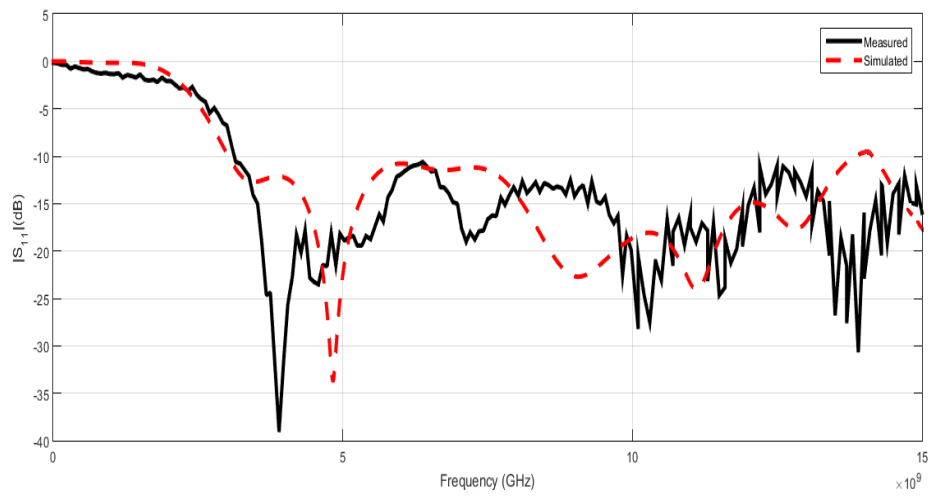


Figure 4.24. Simulated and measured curves of return loss for the Corrugated PCMA.

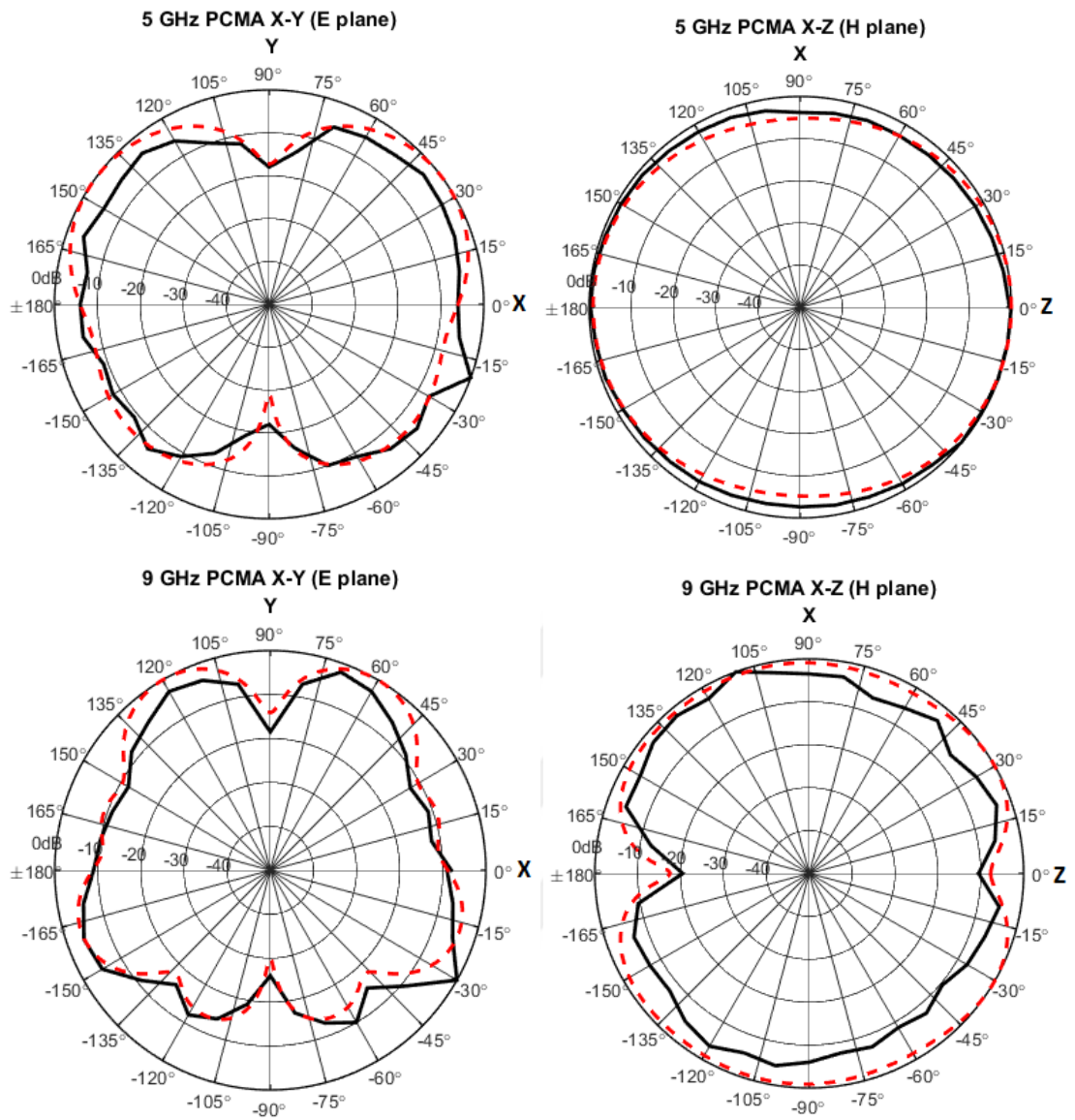


Figure 4.25. Radiation patterns simulated (---) and measured (—) of the PCMA in H and E planes, for frequencies of 5 and 9 GHz.

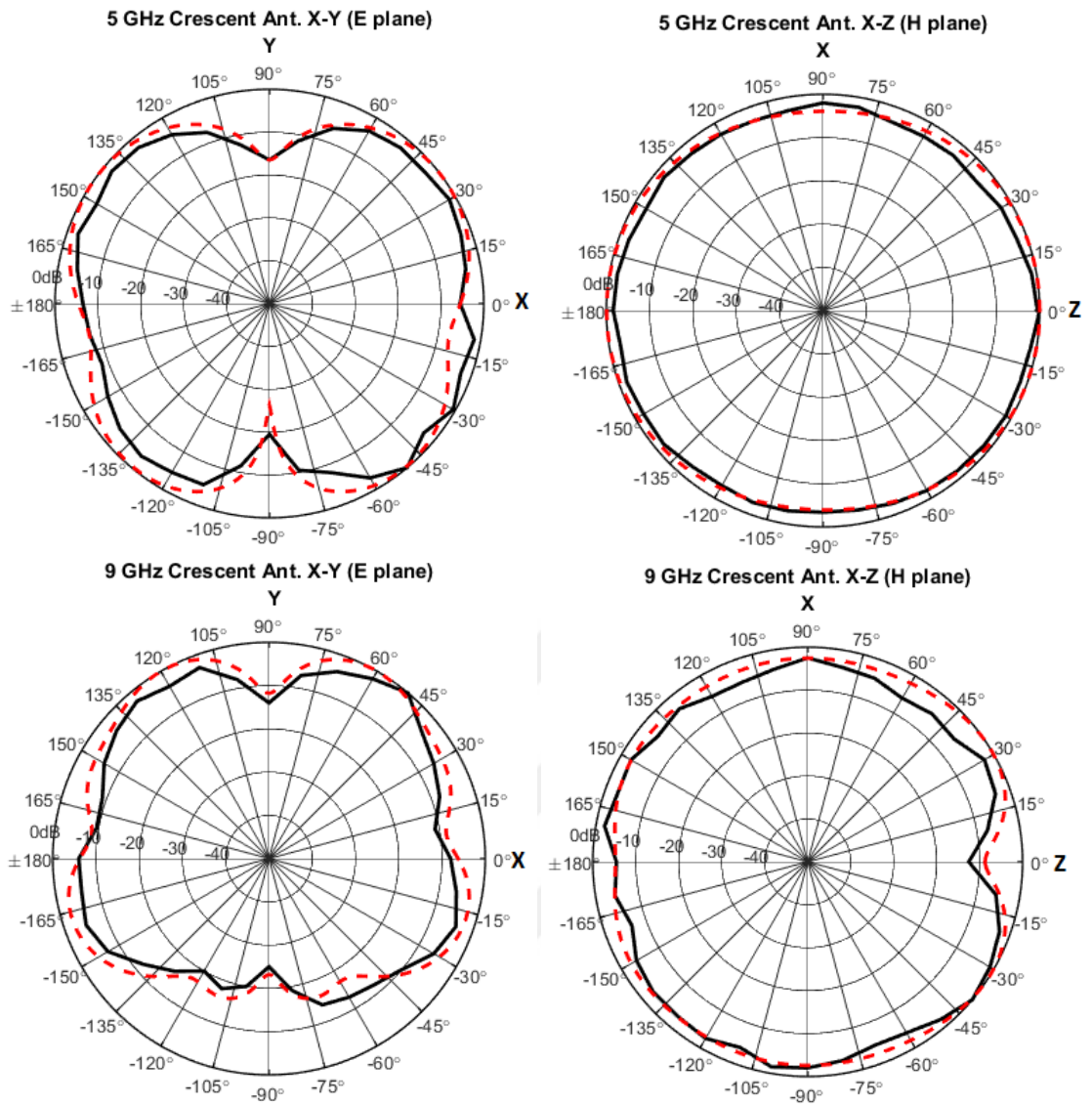


Figure 4.26. Radiation patterns simulated (---) and measured (—) of the PCSMA in H and E planes, for frequencies of 5 and 9 GHz.

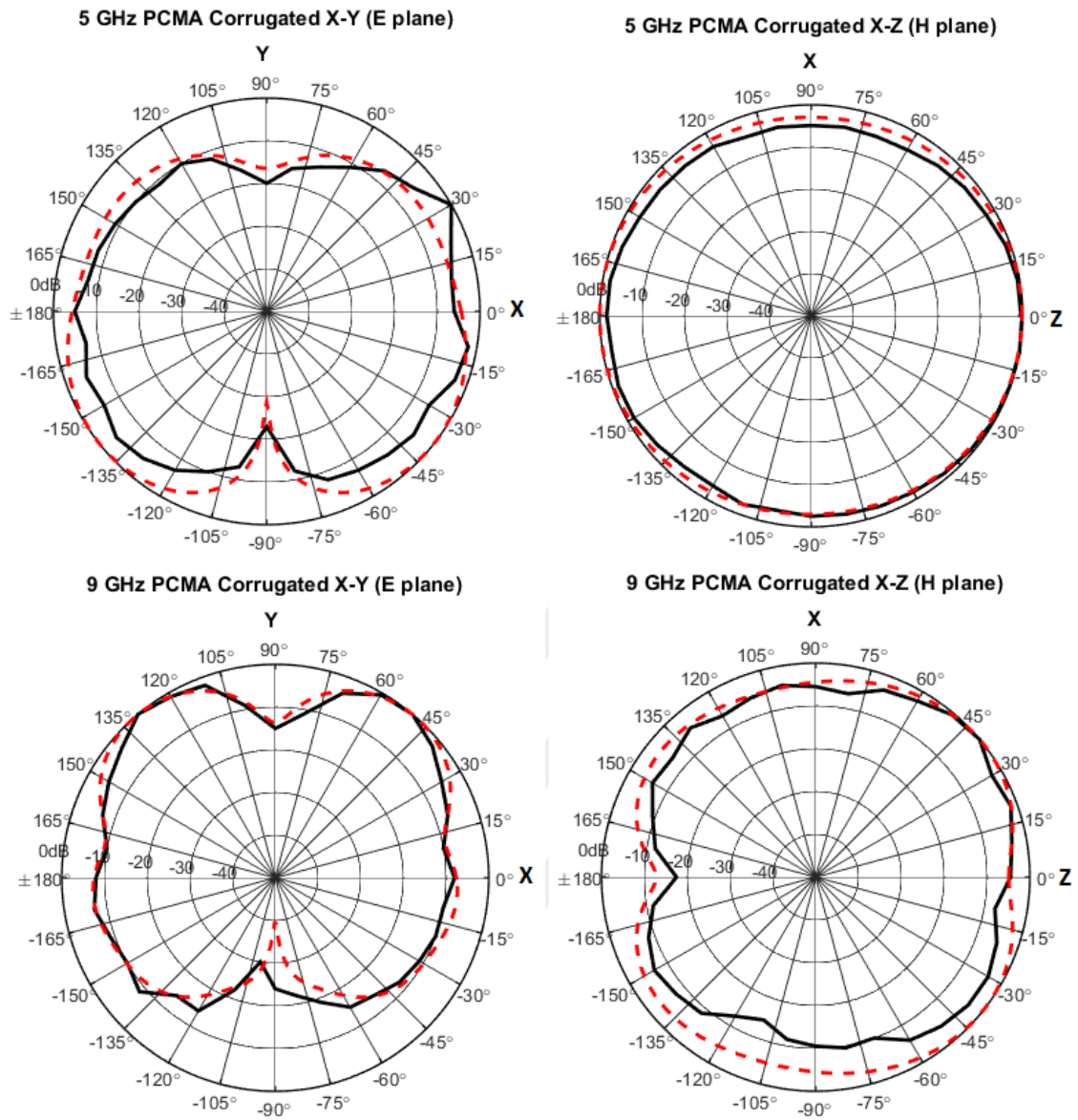


Figure 4.27. Radiation patterns simulated (---) and measured (—) of the Corrugated PCMA in H and E planes, for frequencies of 5 and 9 GHz.

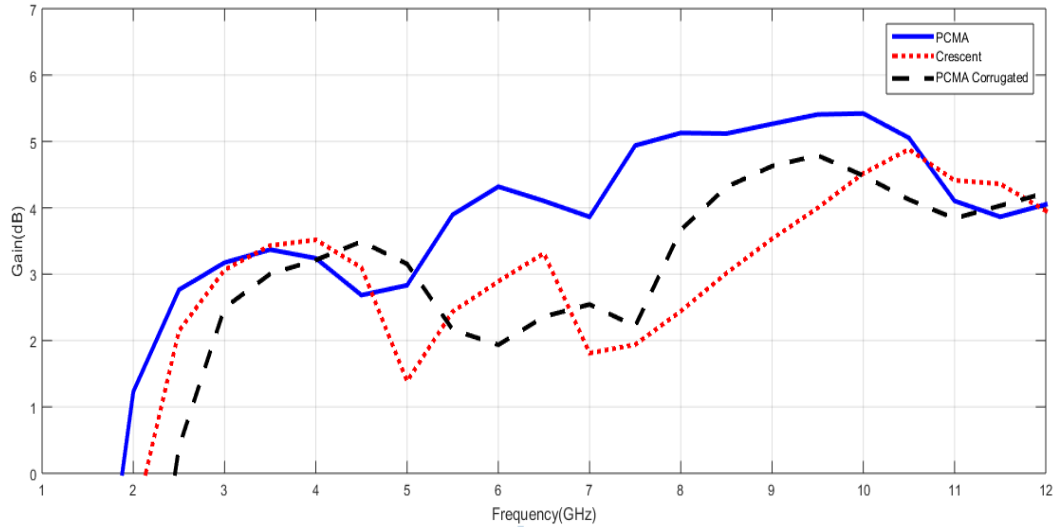


Figure 4.28. Comparison of simulated realized gain curves for the PCMA, PCSMA and corrugated PCMA.



5. CONCLUSIONS AND FUTURE WORKS

5.1. Conclusions

The miniaturization of planar strip-shape monopole antenna (PSSMA) has been introduced via two efficient methods. The first one has been performed via corrugating the edges of the strip-shape radiator element. While the second technique suggested meandering its radiator. Simulation and measurement results showed that both techniques succeeded in reducing the total size of this antenna. The size reduction for the corrugation technique reached 89.3% of reduction with respect to the original parent antenna (*i.e.* the PSSMA), whereas in meandering technique the size reduction was 85.7% of the parent antenna. According to the gathered results it has been concluded that meandering technique gains some advantage on the other technique because the reduction in size was done by 14.28% unlike that of 10.7% for the other technique. Another advantage found by getting a dual-band resonating via meandering which enables working on dual-band of WLAN (*i.e.* 2.45 GHz and 5.5 GHz).

The corrugation technique has also been applied on PCMA antenna which generated a 57.4% of overall size reduction while its gain was still maintaining more than (2 dB), which is comparable with that of half wave dipole antenna. In addition, another technique of miniaturization has been suggested to modify the PCMA antenna by eliminating the least current distributed areas, which resulted in a crescent-shaped radiator, with a 88.2% of overall size reduction. The results have shown that corrugation technique was more efficient due to the reduction in size was done by 42.6% which is more than 11.8% for the other techniques. Simulation results shown that the gain curves for corrugation technique was better than that of area eliminating technique, and the reason may be back to maintaining the perimeter electrical length in corrugated PCMA as much as the physical one of original PCMA antenna, while in PCSMA a certain portion of the perimeter's upper side has been truncated. However, both miniaturized antennas still have the required characteristics just like the original parent PCMA antenna that obeys the UWB requirements.

5.2. Future Works

After completion of this research some ideas could be postponed to next steps as future works which are listed as follow:

1. The adopted techniques of miniaturization can be extended to some other types of antennas like RFID antennas, especially that the size of these antennas is required to be miniaturized which enables compacting within small ID cards or tags.
2. The technique of area elimination is looking very promising, especially for vast types of UWB antennas. So it may be extended to other types of these antennas.
3. Investigating the common features between the design procedure of fractal antennas and the area elimination technique. Especially, that fractal antennas have many eliminating areas.



6. REFERENCES

- Abbosh, A. M. (2009). Miniaturized microstrip-fed tapered-slot antenna with ultrawideband performance. *IEEE Antennas and wireless propagation letters*, 8, 690-692.
- Ahirwar, S. D., & Sairam, C. (2010). Broadband corrugated square-shaped monopole antenna. *ISRN Communications and Networking*, 2011.
- Alam, M. S., Islam, M. T., & Misran, N. (2012). A novel compact split ring slotted electromagnetic bandgap structure for microstrip patch antenna performance enhancement. *Progress In Electromagnetics Research*, 130, 389-409.
- Anguera, J., Martínez, E., Puente, C., Borja, C., & Soler, J. (2004). Broad-band dual-frequency microstrip patch antenna with modified Sierpinski fractal geometry. *IEEE Transactions on Antennas and Propagation*, 52(1), 66-73.
- Azenui, N. C., & Yang, H. Y. D. (2007). A printed crescent patch antenna for ultrawideband applications. *IEEE Antennas and Wireless Propagation Letters*, 6, 113-116.
- Balanis, C. A. (2005). *Antenna Theory: Analysis and Design* 3rd edition John Wiley & Sons. Inc., Publication.
- Balanis, C. A. (2008) *Modern Antenna Handbook*. Hoboken, New Jersey, John Wiley & Sons, pp. 26.
- Bazrkar, A., Gudarzi, A., & Mahzoon, M. (2012). Miniaturization of Rectangular Patch Antennas Partially Loaded with μ -Negative Metamaterials.
- Bead'a, J. M., Abbosh, A. M., Mustafa, S., & Ireland, D. (2014). Microwave system for head imaging. *IEEE Transactions on Instrumentation and Measurement*, 63(1), 117-123.
- Best₁, S. R. (2002). On the significance of self-similar fractal geometry in determining the multiband behavior of the Sierpinski gasket antenna. *IEEE Antennas and wireless propagation letters*, 1(1), 22-25.
- Best₂, S. R. (2002). Operating band comparison of the perturbed Sierpinski and modified Parany Gasket antennas. *IEEE antennas and wireless propagation letters*, 1(1), 35-38.
- Bhuptani, M., & Moradpour, S. (2005). *RFID field guide: deploying radio frequency identification systems*. Prentice Hall PTR.
- Bialkowski, M. E., Abbosh, A. M., Wang, Y., Ireland, D., Bakar, A. A., & Mohammed, B. J. (2011, December). Microwave imaging systems employing cylindrical, hemispherical and planar arrays of ultrawideband antennas. In *Microwave Conference Proceedings (APMC), 2011 Asia-Pacific* (pp. 191-194). IEEE.
- Chakraborty, M., Rana, B., Sarkar, P. P., & Das, A. (2012). Size reduction of a rectangular microstrip patch antenna with slots and defected ground structure.
- Chareonsiri, Y., Thaiwirot, W., & Akkaraekthalin, P. (2017). Design of Ultra-Wideband Tapered Slot Antenna by Using Binomial Transformer with Corrugation. *Frequenz*.

- Chen, M. S., Weng, W. C., & Wang, S. T. (2013, February). Design of the crescent-shape planar ultrawideband antenna with a band-notch structure. In *Next-Generation Electronics (ISNE), 2013 IEEE International Symposium on* (pp. 271-274). IEEE.
- Deschamps, G. A., & Sichak, W. (1953, October). Microstrip microwave antennas. In *third USAF Symposium on Antennas* (Vol. 84).
- El Misilmani, H. M., Al-Husseini, M., Kabalan, K. Y., & El-Hajj, A. (2012). A simple miniaturized triple-band antenna for WLAN/WiMAX applications. *PIERS Proceedings, Moscow, Russia*, 608-612.
- Fadhel, Y. A., & Sayidmarie, K. H. (2012). A Novel UWB Impedance Matching for Planar Circular Monopole Antenna Via Meandering the Microstrip Feed Line. In *Antennas and Propagation Conference (LAPC), Loughborough*.
- Fadhel, Y. A. (2013, July). Design and Implementation of Ultra Wide Band Antennas for Imaging Applications. PhD Thesis, University of Mosul.
- Federal Communications Commission. (2002). In the matter of revision of part 15 of the commission's rules regarding ultra-wideband transmission systems. First Report and Order in ET Docket 98-153.
- Garg, R. (2001). *Microstrip antenna design handbook*. Artech house.
- Hanae, E., Amar Touhami, N., & Mohamed, A. (2015). Miniaturized microstrip patch antenna with spiral defected microstrip structure. *Progress In Electromagnetics Research Letters*, 53, 37-44.
- John L. Volakis. (2007) *Antenna Engineering Handbook, Fourth Edition*.
<http://www.globalspec.com/reference/53296/203279/chapter-8-slot-antennas>.
- Majeed, A. H., Sayidmarie, K. H., Abdussalam, F. M. A., Abd-Alhameed, R. A., & Alhaddad, A. (2015, September). A microstrip-fed pentagon patch monopole antenna for ultra wideband applications. In *Internet Technologies and Applications (ITA), 2015* (pp. 452-456). IEEE.
- Matin, M. A. (Ed.). (2011). *Ultra Wideband Communications: Novel Trends-Antennas and Propagation*. InTech.
- Milligan, T. A. (2005). *Modern antenna design*. John Wiley & Sons.
- Nikolaou, S., & Abbasi, M. A. B. (2016). Miniaturization of UWB Antennas on Organic Material. *International Journal of Antennas and Propagation*, 2016.
- Pandhare, R. A., Zade, P. L., & Abegaonkar, M. P. (2015). Miniaturized Microstrip Patch Antenna Array at 3.8 GHz for WiMax Application.
- Paul Wade. (2001) *The W1GHZ Online Microwave Antenna Book chapter seven part one*. http://www.qsl.net/n1bwt/ch7_part1.pdf
- Puente, C., Romeu, J., Pous, R., & Cardama, A. (1997). Multiband fractal antennas and arrays. In *Fractals in engineering* (pp. 222-236). Springer London.

- Ray, K. P. (2008). Design aspects of printed monopole antennas for ultra-wide band applications. *International Journal of Antennas and Propagation*, 2008.
- Sanghera, P. (2007). *RFID+: CompTIA RFID+ Study Guide and Practice Exam*.
- Sanghera, P. (2011). *RFID+ Study Guide and Practice Exams: Study Guide and Practice Exams*. Syngress.
- Sayem, A., & Ali, M. (2006). Characteristics of a microstrip-fed miniature printed Hilbert slot antenna. *Progress In Electromagnetics Research*, 56, 1-18.
- Sayidmarie, K. H., & Fadhel, Y. A. (2011). Self-complementary circular disk antenna for UWB applications. *Progress In Electromagnetics Research C*, 24, 111-122.
- Sayidmarie, K. H., & Fadhel, Y. A. (2012, November). Design aspects of UWB printed elliptical monopole antenna with impedance matching. In *Antennas and Propagation Conference (LAPC), 2012 Loughborough* (pp. 1-4). IEEE.
- Singh, K., Grewal, V., & Saxena, R. (2009). Fractal antennas: a novel miniaturization technique for wireless communications. *International Journal of recent trends in Engineering*, 2(5), 172-176.
- Stutzman, W. L. (1981). *Antenna Theory and Design*. Hoboken, New Jersey, John Wiley & Son.
- Wadell, B. C. (1991). *Transmission line design handbook*. Artech House.
- Wheeler, H. A. (1977). Transmission-line properties of a strip on a dielectric sheet on a plane. *IEEE Transactions on Microwave Theory and Techniques*, 25(8), 631-647.
- Zhao, K., Ying, Z., & He, S. (2015, May). Antenna designs of smart watch for cellular communications by using metal belt. In *Antennas and Propagation (EuCAP), 2015 9th European Conference on* (pp. 1-5). IEEE.

CURRICULUM VITAE

PERSONAL INFORMATION

Name and Surname : Revink M. Abdulhakim
Birth Date and Place : 14/12/1990 Iraq, Duhok
Telephone : 009647504500106
Email : revinkmasoud@gmail.com

EDUCATION

Degree	Name, Country, Province	Graduation Year
High school	: Alla Secondary School, Iraq, Duhok	2008
University	: University of Duhok, Iraq, Duhok	2013
M.Sc.	: Siirt University, Turkey, Siirt	2017

WORK EXPERIENCES

Year	Institution	Duty
2013-2014	Duhok Gas Power Station	Maintenance Engineer
2014-till now	Nawroz University	Teaching Assistant

SPECIALTY AREA

Electrical and Computer engineering

FOREIGN LANGUAGES

English (good)
Arabic (very good)
Turkish (medium)

OTHER FEATURES YOU WANT TO SPECIFY

Power and Control engineering

PUBLICATIONS

Some of the miniaturized antennas have been introduced in this publication:

Conference Paper

YASSER A. FADHEL, MUSA ATAŞ, and REVINK M. ABDULHAKIM,
“Miniaturization of A Planar Strip-Shaped Monopole Antenna for WLAN Application”,
Proceedings of ICRIE2017, Duhok, Iraq, 26-27 Apr. 2017.